Development of Waste Tire Gasification Processes to Methanol with Comparative

Lifecycle Assessment

Kashish Shah

A Thesis

in

the Department

of

Chemical and Materials Engineering

Presented in Partial Fulfillment of the Requirements

For the Degree of Master of Applied Science at

Concordia University

Montreal, Quebec, Canada

October 2023

CONCORDIA UNIVERSITY
School of Graduate Studies

This is to certify that the thesis prepared

By: Kashish Shah

Entitled: Development of Waste Tire Gasification Processes to Methanol with

Comparative Life Cycle Assessment

and submitted in partial fulfilment of the requirements for the degree of

Master of Applied Science (Chemical and Materials Engineering)

complied with the regulations of the University and meets the accepted standards with respect to originality and quality.

Signed by the final Examining Committee:

                            Chair
         Dr. Melanie Hazlett

                            Examiner
         Dr. Ivan Kantor

                            Supervisor
         Dr. Yaser Khojasteh

Approved by
      Dr. Sana Jahanshahi Anbuhi, Graduate Program Director

October 2023
      Dr. Mourad Debbabi, Dean Gina Cody School of Engineering and Computer Science

ABSTRACT

Development of Waste Tire Gasification Processes to Methanol with Comparative
Lifecycle Assessment

Kashish Shah

This thesis presents an innovative approach to the escalating global issue of waste tire accumulation, focusing on the design and development of a novel waste tire (WT) electrified gasification process for methanol production. The proposed solution addresses the environmental impacts of existing recycling methods and offers a greener alternative. The study involves a comparative analysis of two primary processes: the conventional waste tire (WT-Conventional) and the proposed waste tire electrified (WT-Electrified) pathways. These processes are designed and simulated using AspenPlus software to ensure accuracy and feasibility.

A comprehensive techno-economic analysis is conducted for both processes, providing an in-depth understanding of their economic viability. Furthermore, this research expands its scope by implementing a Life Cycle Assessment (LCA) performed through OpenLCA software. The LCA results not only facilitate a comparison between different electricity generation sources but also benchmark the proposed pathway against other conventional routes for methanol production.

The research findings reveal promising results for the WT-Electrified process. Key performance indicators such as thermal efficiency, CO_2 emissions, and economic analysis demonstrate its potential superiority over the conventional counterpart. This thesis underscores the potential of the WT-Electrified gasification process as an environmentally-friendly and economically viable solution for waste tire management. It provides a solid foundation for further exploration and refinement, paving the way towards a more sustainable future.

Acknowledgements

I extend my profound gratitude to my supervisor, Dr. Yaser Khojasteh, whose support and immense knowledge have been beneficial in conducting my research and writing this thesis. His guidance has been invaluable, and I am immensely thankful for his contributions.

I am also deeply grateful to the examining committee and the Department of Chemical and Materials Engineering at Concordia University for their constructive feedback and academic support throughout my research journey. I would also like to thank my co-supervisor and teammate, Khadijeh Barati, for her unwavering assistance during my research. Similarly, I must appreciate my CSTAR teammates, who provided optimal solutions and helped me overcome challenges during team meetings.

On a personal note, I owe a debt of gratitude to my parents, Mr. Jayesh Shah and Mrs. Nisha Shah. Their endless love and support have been my rock, enabling me to pursue and successfully complete my Master's degree. My sister, Anokhi's motivation and belief in me have been a source of constant inspiration, for which I am eternally grateful.

Lastly, I want to express my heartfelt thanks to my friends for their unwavering support and motivation. They have been my pillar of strength, and their encouragement has played an instrumental role in my academic journey.

To all mentioned above and those who have contributed indirectly, your collective inputs have made this achievement possible. Thank you!

Table of Contents

List of Figures

List of Tables

Nomenclature

WT	Waste tires
MVR	Mechanical vapor recompression
SMR	Steam methane reforming
GHG	Greenhouse gas
GTR	Ground tire rubber
WTE	Waste tire electrified
WTC	Waste tire conventional
PEM	Proton exchange membrane
LHV	Lower heating value
PFD	Process flow diagram
HPS	High pressure steam
BFW	Boiler feed water
ASU	Air separation unit
COS	Carbonyl Sulphide
DGA	Diglycolamine
SN	Stoichiometric number
LCA	Life cycle assessment
TRACI	Tool for reduction and assessment of chemicals and other environmental impacts
NG	Natural gas
CEPCI	Chemical engineering plant cost index
MSP	Minimum selling price

Chapter 1 – Electrification in the chemical industry

1. Introduction

Addressing the global challenge of cutting carbon emissions while maintaining our quality of life is especially tough for industries that heavily rely on burning fossil fuels. These sectors mainly rely on fossil fuels because they are easily available, affordable, and have high energy density. However, this reliance makes it difficult to aim for net-zero carbon emissions by 2050. Nonetheless, this ambitious objective remains feasible through the substitution of traditional fossil fuel combustion with sustainable renewable electricity sources [1]. It is worth noting, however, this transition is not without its challenges. Electricity generation and distribution can incur energy losses, which might seem less efficient than directly burning fuels for heat [2]. Despite this, a carbon-neutral future, particularly for major industries, depends on embracing renewable energy sources and thereby necessitating innovative strategies to address these complex challenges.

Renewable energy sources like water (hydro) and wind are becoming more popular. They are preferred over fossil fuels because of their positive environmental impact, lower electricity expenses, and the prospect of saving costs associated with potential carbon taxes.Eryazici et al. highlighted that the widespread adoption of renewable electricity could yield a substantial 35% reduction in carbon emissions within the chemical industry, primarily attributed to its application in electricity-intensive processes [3]. These processes, such as reforming, gasification, and steam cracking, crucially involve high-temperature requirements and are pivotal in generating essential chemicals like methanol, ammonia, and olefins, serving as raw materials or feedstocks for diverse chemical applications [3]. Traditionally, fulfilling this energy demand requires the combustion of carbon-based fuels, a practice that emits greenhouse gases (GHGs) and amplifies concerns regarding climate change [4]. Transitioning toward renewable electricity offers a promising avenue to mitigate these environmental challenges while sustaining critical industrial processes.

Different electrification technologies exist for decarbonizing chemical processes, which vary based on the temperature requirements. In this study, the term "decarbonizing" refers to the process of reducing environmental carbon dioxide emissions. This objective can be accomplished by either avoiding carbon dioxide emissions or by capturing carbon dioxide and utilizing it to synthesize valuable chemicals [4]. For low-temperature processes such as those operating below 200°C,

reducing carbon emissions by adapting to a cleaner process. On the other hand, high-temperature reactors, which operate above 500°C, require electrification technologies that can withstand high temperatures for chemical reactions. A brief explanation of the electrification technology currently used in low-temperature and high-temperature processes has been given below.

1.1. Low-temperature processes

Thermal energy can be further divided into four end-use categories: process heating, process cooling, space heating, and space cooling [5]. Figure 1 presents the total industrial process heat demand by temperature level. Low-temperature reactors usually work with temperatures <200°C, which has a heating demand of 37% of the total process heat requirement [5].
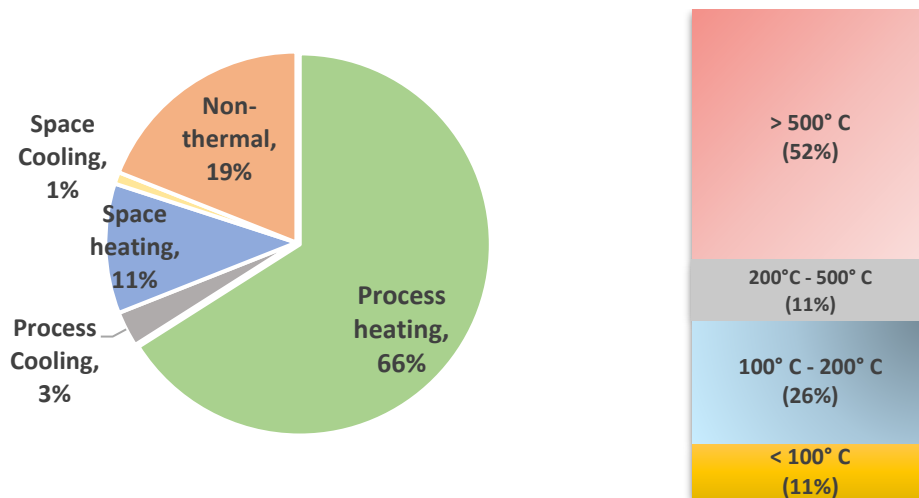
Figure 1: Energy demand by European industries by its application (left) and process heating demand by temperature level (right) [5]

1.1.1. Industrial Heat Pump and Mechanical vapor recompression (MVR)

The adoption of heat pumps and mechanical vapor recompression (MVR) in the industrial sector signifies a pivotal movement towards greener and more efficient methodologies. The inclusion of heat pumps and MVR stands out as a key strategy for the electrification of low-temperature reactors. Heat pumps transfer heat from a low-temperature source to a high-temperature sink. They use a refrigeration cycle that consists of a compressor, evaporator, condenser, and expansion valve. The refrigerant in the system absorbs heat from the low-temperature source, evaporates, and is

then compressed to high pressure and temperature, releasing heat to the high-temperature sink [6]. Take the dairy industry, for example: when milk is cooled down, a significant amount of heat is typically lost. Nevertheless, with heat pumps, this otherwise wasted energy is harnessed and repurposed to preheat water, leading to notable energy savings [7].

On the other hand, MVR is a process that uses a compressor to increase the temperature and pressure of a vapor stream, which then condenses to release heat. MVR is commonly used for evaporating and concentrating liquids [8]. By doing this, MVR allows industries to reuse the same vapor multiple times, making processes more energy efficient. MVR finds significant application in industries where evaporation plays a crucial role. For instance, in the desalination industry, where seawater is turned into fresh water, a lot of energy is traditionally needed to boil the water and produce vapor. With MVR, the steam generated from seawater boiling is compressed to increase its temperature. This hotter steam can then be used again to heat the next batch of seawater, reducing the amount of new heat needed [9]. This makes the whole process more energy-efficient and cost-effective. Several works have been done on incorporating heat pumps and MVRs to supply the energy demand of the chemical processes. For instance, Ai et al. [8] studied MVR for solution regeneration and reached the conclusion that MVR offers significant energy savings compared to other technologies. Specifically, MVR can achieve energy savings of 35.7%, 73.5%, and 91.2% compared to air-driven heat pumps, three-effect evaporating systems, and single-effect evaporating systems, respectively.

1.2. High-temperature processes

High-temperature processes that operate above 200°C dominate industrial heat needs, accounting for a substantial 63% of the total demand (Figure 1). However, the energy to fuel processes primarily comes from burning fossil fuels, with a whopping 78% reliance [5]. Despite the clear inclination towards fossil fuels, there is a silver lining; the use of electricity in industries has been on a steady rise, now accounting for approximately 20% of the total energy requirements [10]. This transition towards electrification is pivotal for several reasons. Primarily, electrifying these processes through renewable electricity has the potential to reduce carbon emissions. Taking a closer look at specific industrial processes, steam methane reforming (SMR) is responsible for 95% of the world's hydrogen production [11]. Currently, SMR is heavily dependent on fossil fuel combustion, i.e. natural gas, resulting in a significant volume of GHG emissions, about 11.5 kg

CO_2 eq./kg H_2 [12]. Wismann et. al. [13], presented an entirely electricity-driven reactor for methane reforming, which eliminates the thermal limitations and, in addition, decreases the reactor volume and waste heat streams. This gives a competitive edge to large-scale production of chemicals like methanol, ammonia, and biofuels.

Some of the new technologies for the electrification of high-temperature reactors are described below:

    (1) Plasma electrified reactor

    (2) Microwave-assisted electrified reactor

1.2.1. Plasma electrified reactor

Plasma is the fourth state of matter, identified by Sir Williams Crookes in 1879, which was then introduced by Irving Langmuir as an ionized gas in 1928. It consists mainly of charged particles like ions and electrons, though the plasma is electrically neutral [14]. Plasma is a highly ionized gas that conducts electricity and can generate its own magnetic fields. It has a low density and can emit light of various colors. Plasma's high temperature and chemical reactivity make it useful in various applications, including energy and materials science. Munir et al. [15] studied plasma gasification of solid waste, which showed plasma gasification can achieve extreme thermal conditions (approximately 2000°C to 14000°C). With the help of steam, hydrogen and carbon dioxide, it converts nitrogen and sulfur in the feed to nitrogen and hydrogen sulfides, eliminating the formation of NO_X and SO_2. However, this approach has not yet been successfully commercialized due to several challenges, including high initial investment and ongoing operational expenses, a restricted understanding of the process, and plasma stability [16].

1.2.2. Microwave-assisted electrified reactor

Microwaves are electromagnetic waves with wavelengths of 1 m to 1 mm and frequency from 300 MHz to 300 GHz comprising of both electric field and magnetic field [17]. Lahijani et al. [18], studied microwave-enhanced CO_2 gasification of palm shells. In comparing the results of microwave gasification to those of thermal gasification, it is found that the production of CO in the former is significantly higher. Specifically, at a temperature of 750°C, the CO production in the microwave-driven reaction is 13.7 times greater than that of thermal gasification. Microwaves have some distinct characteristics that make them an efficient heating technique. They can heat

substances rapidly and selectively, and they do not affect the rate of chemical reactions [17]. However, this method has many operational challenges, such as its functioning at varying temperatures due to its electromagnetic properties, and also construction and maintenance of the reactor would be a challenge.

1.3. Summary

In reviewing the various electrification technologies available, it is clear that their suitability varies based on the temperature needs of different processes. For those operating at lower temperatures, tools like heat pumps and MVR are effective in conserving energy and reducing carbon emissions since they reduce fossil fuel use. Alternatives like microwave or plasma-driven reactors can be employed for the high-temperature processes, sidestepping the traditional thermal reactors. This research will explore a novel microwave-powered high-temperature reactor designed to break down hydrocarbons and produce syngas. The main goal is to evaluate the energy efficiency of this electric microwave reactor in comparison to its traditional counterpart.

Chapter 2: Waste Tire Recycling

2. Waste Tires

The average lifespan of tires is about 80000 km, but the lifespan varies with different tire manufacturers, depending on the workload, driving behavior, and road condition. It is estimated that 1.6 billion new tires are generated yearly, and 1 billion waste tires are generated. In 2019, the United States generated approximately 4.46×10^6 tonnes of waste tires [19], and Canada collected about 4.46×10^5 tonnes of waste tires in 2020 [20]. The majority of these waste tires are dumped in landfills due to the high cost involved in the recycling process. Disposing of waste tires in open landfills poses difficulties in terms of degradation, and methods like combustion or incineration can result in the emission of toxic gases that have adverse environmental effects [21]. The recycling of waste tires is a challenging task due to their shapes, size, composition and cost associated with it [22]. A major problem for recycling is vulcanized rubber as it is composed of a long chain of polymers that are crosslinked, with the addition of sulfur, carbon and other chemicals to increase its durability [23].

Data collected by the U.S. Tire Manufacturers Association [24] shows that 17% of waste is dumped in landfills, but about 83% of waste tires are recycled in many different ways, such as retreading and incineration for energy recovery, pyrolysis for gas oil and char recovery [22]. It's difficult to decompose rubber tire as a whole. Thus, to overcome this challenge waste tires are crushed into small particles to form ground tire rubber (GTR), which are easy to process [25].

Every tire manufacturer has its unique composition, so it is difficult to know the exact composition of each tire so that the average composition of the scrap tires has been taken into account which is shown in Table 1.

Table 1: Typical composition of passenger and truck tires [26].

Component	Passenger tire (wt.%)	Truck tire (wt.%)	Comments
Rubber	47	45	Many different synthetic and natural rubbers are used, e.g. stirene-butadiene rubber, natural rubber (polyisoprene), nitrile rubber, chloroprene rubber, polybutadiene rubber
Carbon black	21.5	22	Used to strengthen the rubber and aid abrasion resistance
Metal	16.5	21.5	Steel belts and cord for strength

Textile	5.5	–	Used for reinforcement
Zinc oxide	1	2	Used (with stearic acid) to control the vulcanization process and to enhance the physical properties of the rubber
Sulphur	1	1	Used to crosslink the polymer chains within the rubber and also to harden and prevent excessive deformation at elevated temperatures
Additives	7.5	5	e.g. Clay or silica used to partial replace carbon black

2.1. Waste tire conversion methods

2.1.1. Retreading

Retreading is a cycle to increase the lifetime of a scrap tire by removing its used tread and applying a new one through cold or hot cycles. Normally, the tire remnants go through a recapping framework to acquaint another track with the tire. The retreading system needs 30% of the energy compared to manufacturing new tires and 25% of the unrefined components needed to deliver another tire. However, this method's limited use is a downside, as this technique only applies to reusing tires that have no body damage and passed a mileage investigation [22,24,25].

2.1.2. Incineration

Incineration is an exothermic process with a temperature above 400°C, used to recover energy from waste tire due to its calorific value (32.6 MJ/kg) and used as a fuel source. Carbon black can also be recovered by incinerating tires [29]. This process has low heat production costs and maximum heat recovery, but the air emissions are also high, which needs to be assessed for environmental impacts [22,27].

2.1.3. Pyrolysis

Widely used method for recycling is the pyrolysis method, which involves the thermal decomposition of the heavy crosslinked hydrocarbons chains present in the tires to generate an oil, gas, and char product at an average pyrolysis temperature ≥400°C. The oil can be utilised as a chemical feedstock. The gases produced by tire pyrolysis are generally composed of C1–C4 hydrocarbons and hydrogen with a high calorific value, indicating that they have enough energy to fuel the pyrolysis process. The carbon black filler and char formed during the pyrolysis of the rubber make up the solid char [26]. The advantages of this process are that it generates a high

product yield of oil, gas, and black carbon, which can be used as a fuel source in small and big scale industries, but this type of process needs a big pyrolysis plant which can be costly [25].

2.1.4. Hydrothermal Liquefaction

Hydrothermal liquefaction (HTL) is a thermal depolymerization process that converts wet feedstock into liquid biofuels. The process involves heating the feed in the presence of water at high temperatures and pressures, typically ranging from 250°C to 550°C and 5 to 25 MPa, respectively [31]. During the process, the waste tires are hydrolyzed, and its organic compounds are broken down into smaller molecules and then converted into a liquid form. The resulting bio-crude oil can be further upgraded to produce transportation fuels such as gasoline, diesel, and jet fuel. HTL has several advantages over other biofuel production methods, including its ability to handle wet feed, its potential to produce high yields of bio-crude oil, and its ability to use a wide variety of feedstocks.

However, the HTL process also has several disadvantages. The main challenge is that the process is energy-intensive, requiring a significant amount of heat to reach the high temperatures and pressures necessary for the reaction. This energy requirement makes the process expensive and limits its scalability. Furthermore, the process requires a constant supply of water, which can be a limitation in water-scarce areas. Additionally, the HTL process generates wastewater that must be treated before disposal, adding to the overall cost of the process. Finally, the bio-oil produced by HTL has some limitations as a fuel, including its high oxygen and water content, which makes it less energy-dense than fossil fuels and limits its shelf-life [29,30].

2.1.5. Gasification

Gasification is the process of reacting a solid feedstock with a gasifying agent such as air, steam, or oxygen under sub-stoichiometric conditions to produce syngas, a mixture of carbon monoxide, hydrogen, and carbon dioxide, as well as other hydrocarbons such as methane and ethane. Syngas can be used to generate power and processed further to produce alternative fuels such as methanol or DME. The solid phase called char, an unconverted fraction of the feedstock during gasification, mainly consists of carbon and ash [14,29].

Conventionally, gasification can be done in different reactors, such as fixed bed reactors and fluidized bed reactors, and at a very high temperature, usually more than 800°C. In the conventional gasification processes, this temperature is achieved by burning fossil fuels, which

emit a significant amount of CO_2 into the atmosphere and consume fossil fuels [35]. Hence, to reduce CO_2 emissions, innovative processes based on electrified heating of high-temperature gasification reactors must be developed to incorporate renewable electricity and achieve a viable route for sustainable fuel and chemical production.

Xie et al. [36] developed a microwave-assisted biomass gasification system. Their study concludes that microwave heating is efficient with the use of Ni/Al_2O_3 catalyst for the production of syngas and tar reduction. They performed an experiment in a microwave oven and quartz reactor with a microwave absorbent bed. The corn stover is selected as feed and gasified at 900°C temperature. While using the nickel-based catalyst, the gas conversion is above 80%. In comparison, the tar content is 7%, and the maximum syngas (H_2 + CO) content is obtained. They have introduced a novel concept of dual fluidized bed gasifiers, primarily designed for commercial applications. This innovative approach can achieve temperatures exceeding 1200°C, producing cleaner gas compared to lower-temperature reactors. Furthermore, this design showcases enhanced energy efficiency.

2.2 Research Objective

This research study on electrified gasification of waste tires introduces a novel method for methanol production, addressing both waste management and sustainable energy challenges. While prior studies have explored waste-to-energy techniques, this work distinctively bridges the scientific gap related to carbon emissions. Optimizing methanol production to minimize these emissions presents a viable solution to reduce tire waste and promote clean energy. Furthermore, the inclusion of a lifecycle assessment ensures a comprehensive evaluation of the environmental impacts of this innovative process.

However, technical and economic challenges must be addressed to make this process economically feasible and environmentally sustainable. This research aims to investigate the technical, economic, and environmental aspects of converting waste tires to methanol and assess this process's potential as a sustainable waste management solution. The findings of this study will contribute to the development of new waste-to-value technologies and support the transition towards a circular economy.

Chapter 3: Process Description and Design

3. Process description

Overall, the WT-electrified process consists of 6 process units, while the conventional process has seven units, which has an additional amine unit designed to capture excess CO_2. Major process units designed in both processes are described below.

- Gasification unit: Waste tires are converted to syngas
- H_2 unit: Hydrogen production using PEM hydrolysis and hydrogen compression
- Gas treatment: To remove impurities and dust particles
  - Clauspol unit: Sulfur recovery from syngas
  - Amine unit (only in conventional process): Syngas treatment and capture of excess CO_2
- MeOH unit: Methanol synthesis, recovery and purification
- Steam generation: Steam is generated from combustion of byproducts to generate electricity

In order to achieve a better understanding of the performance of the proposed electrified gasification process, the process design and simulation are conducted for both the electrified reactor as well as the conventional thermal reactor. The simplified BFD of the electrified-WT gasification process and conventional-WT gasification process are shown in Figure 2 and Figure 3, respectively. The process simulation is conducted using Aspen Plus v12.1 software. The process of converting waste tires into valued products involves several stages, starting with pre-treatment. In this stage, the tires are shredded into smaller pieces in the size of 0.18 mm and cleaned of any contaminants such as dirt, rocks, or metal pieces such as metal wires are removed. The tire pieces are then fed into the gasification section, where they are exposed to high temperatures of 1100°C. At this temperature, the tire pieces decompose, resulting in syngas and carbon residue production. The carbon residue produced during the gasification process is also utilised in other industries, such as in producing activated carbon for water purification and air filtration systems [37]. The syngas is then sent to the gas cleanup section, where any acid gases such as carbon dioxide and hydrogen sulfide are removed. This guarantees the production of high-quality syngas while ensuring that sulfur emissions remain within permissible levels [38]. The next stage involves the production of methanol from the syngas through a series of chemical reactions that convert the

syngas into methanol. The simulation results will be utilised for lifecycle assessment and economic analysis of both processes.
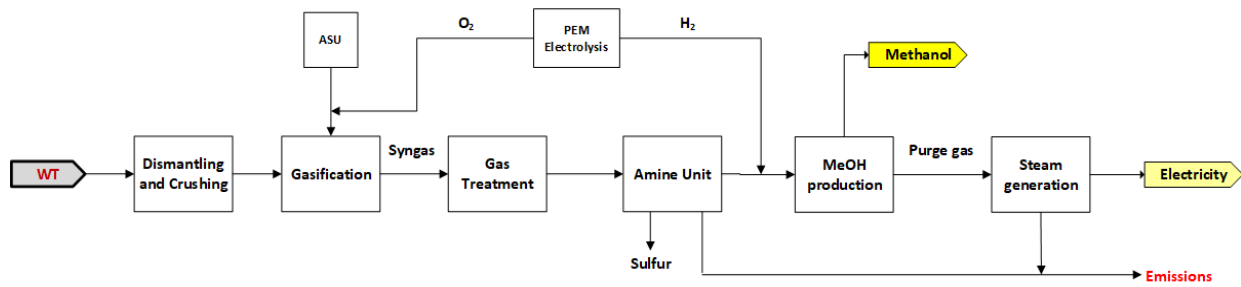

Figure 2: Block flow diagram of the WT-conventional conversion process
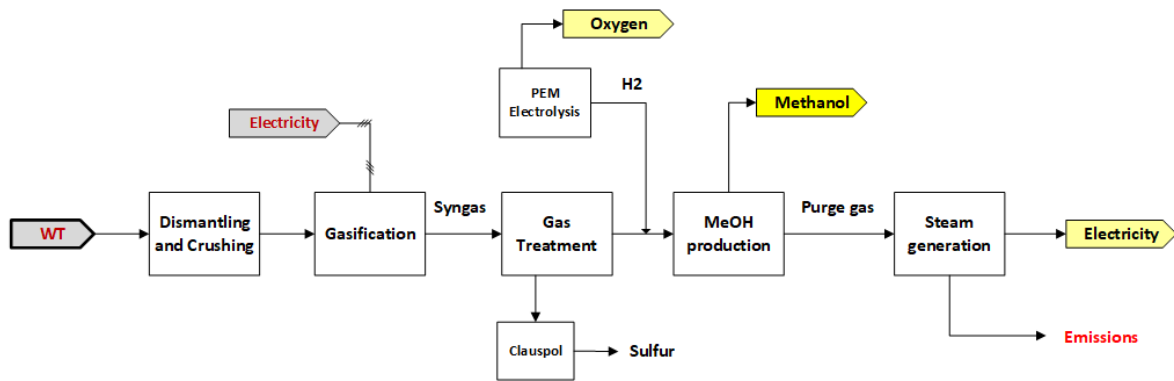

Figure 3: Block flow diagram for the WT-electric process

3.1. Tire feedstock

This study focuses on discarded tires from all over Canada, but managing such a vast amount of tire waste nationwide is a significant challenge when it comes to precise assessment and handling. The difficulty arises because there is a wide variety of tire types, making it challenging to evaluate their characteristics collectively. Consequently, we are concentrating on the standard composition of tires typically used for passenger vehicles. In Table 2, the typical composition of waste tires is listed. The electricity load for grinding is calculated based on the correlations in Ref. [39].

Table 2: Feedstock composition

Unit	Parameters	References
Waste tires	Mass flow rate = 50,000 kg/h LHV – 33.96 MJ/kg **Ultimate (wt%):** Carbon: 77.3 Hydrogen: 6.2 Nitrogen: 0.6 Sulfur: 1.8 Oxygen: 7.3 Ash: 6.8 **Proximate (wt%):** Volatile Matter (VM): 67.7, Fixed Carbon (FC): 25.5, Ash: 6.8	[40]
Waste tire pre-treatment	Crumb size = 0.18mm	[3,4]

3.1.2. Process assumptions

Mass and energy balances were conducted using Aspen Plus software. In both WTE and WTC processes, the Peng-Robinson with Boston-Mathias (PR-BM) thermodynamic property is used for the physical calculations for most of the units as it is a recommended property for high-pressure hydrocarbons applications, especially for gas processing [42]. The UNIQUAC with Redlich-Kwong (UNIQ-RK) model and STEAMNBS model were used for the methanol production and steam generation units. The amine unit in the WTC process uses the ELECNRTL electrolyte package, which is considered the most versatile method for managing electrolyte properties. It can handle low and high concentrations, as well as it is effective for both aqueous and mixed solvent systems [42]. The ASPEN simulation did not incorporate the modeling of specific units, such as the Clauspol unit for sulfur removal, the ASU unit for oxygen production, and the PEM electrolyzer for hydrogen production. Instead, critical design parameters, including oxygen purity, hydrogen purity, and electricity consumption, were sourced from a comprehensive literature review and are detailed in the table below for reference. The detailed design parameters and specifications are listed in Table 3.

Table 3: Design parameters and specifications

Unit	Description
Gasification	
Gasification temperature	1100°C
Air Separation Unit (ASU)	
Oxygen purity	99.5% [43]
Electricity demand	245 kWh/tonne O_2 [44]
Gas Treatment	
Carbonyl Sulphide (COS) hydrolysis reactor	100% COS conversion [45]
Acid gas removal column	
	No. of stages = 30
Amine column	CO_2 in clean gas< 5%
	No. of stages = 30
	DGA recovery = 99.99%
Hydrogen Production	
Electrolysis process	Proton Exchange Membrane (PEM)
Electricity consumption (kWh/kg H_2)	52.37 [46]
MeOH production	
First Stage reactor	
Residence time (sec)	6.3
Velocity (m/s)	0.8
Second stage reactor	
Residence time (sec)	10.8
Velocity (m/s)	0.46
First Column	
Methanol mass recovery	99.7%
	No. of stages= 30
Second Column	
Methanol purity (%mass)	99.85 [47]
	No. of stages= 45
Methanol mass recovery	99.7%
Power generation	
Boiler's excess inlet oxygen	5% [48]

3.2. Gasification

Figure 4 shows the process flow diagram of the gasification unit. The grounded waste tire feed is directed to the RYIELD block, where non-conventional feed undergoes decomposition into reactive compounds specified by the calculator block based on the ultimate analysis of the tires. Subsequently, the gasification reactions are simulated using an RGIBBIS reactor, which minimizes the Gibbs free energy assuming chemical equilibrium conditions. The following reactions take place in the gasifier [40]:
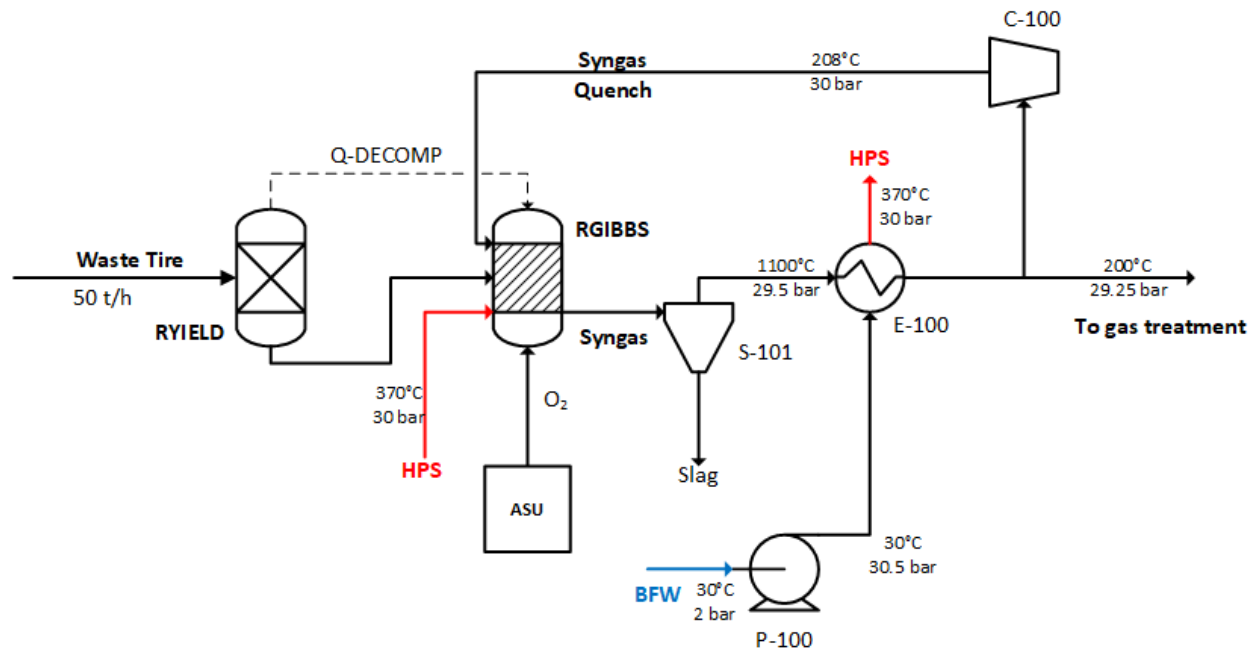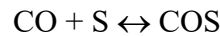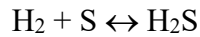
$$C + O_2 \leftrightarrow CO_2$$

$$C + CO_2 \leftrightarrow 2CO$$

$$CO + 3H_2 \leftrightarrow CH_4 + H_2O$$

$$CO + H_2O \leftrightarrow H_2 + CO_2$$

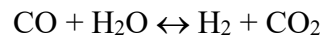$$H_2 + S \leftrightarrow H_2S$$

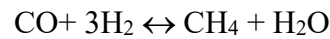$$CO + S \leftrightarrow COS$$
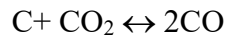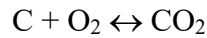
Figure 4: Process flow diagram of the gasification unit

Figure 5 shows the gasifier reactors used in both WT-conventional and WT-electrified processes. A typical shell gasifier model has been selected for this study, as the shell gasifier technology uses a dry-feed, entrained flow gasifier which operates for a wide variety of feedstocks [49]. For high temperatures and pressure, entrained gasifier is most suitable for dry feedstocks [50]. Ground

14

waste tires are fed into the gasifier with the help of HPS, and feed is reacted at 1100°C, which at this high temperature, the reaction instantly becomes equilibrium. Raw syngas leaves the gasifier at a relatively high temperature and is sent to the syngas cooler. Syngas cooler is an integral part of the gasifier used for heat recovery and superheated high-pressure steam generation.

Syngas leaving from the gasifier is at a very high temperature. To prevent the damage of the latter equipment, the syngas is rapidly cooled down using quench syngas at the gasifier exit. Following this, the syngas is channelled through the transfer duct to a syngas cooler. Here, in this heat exchanger, the syngas undergoes further cooling, producing saturated steam in the process. By the time syngas exits the cooler, its temperature is reduced to 200°C.

In the electrified-WT gasification process, the reactor operates solely using electricity, employing microwave heating technology to gasify the feed material in the presence of microwave radiation. In contrast, the conventional-WT gasification process relies on the combustion of oxygen generated from an ASU, as depicted in Figure 5.
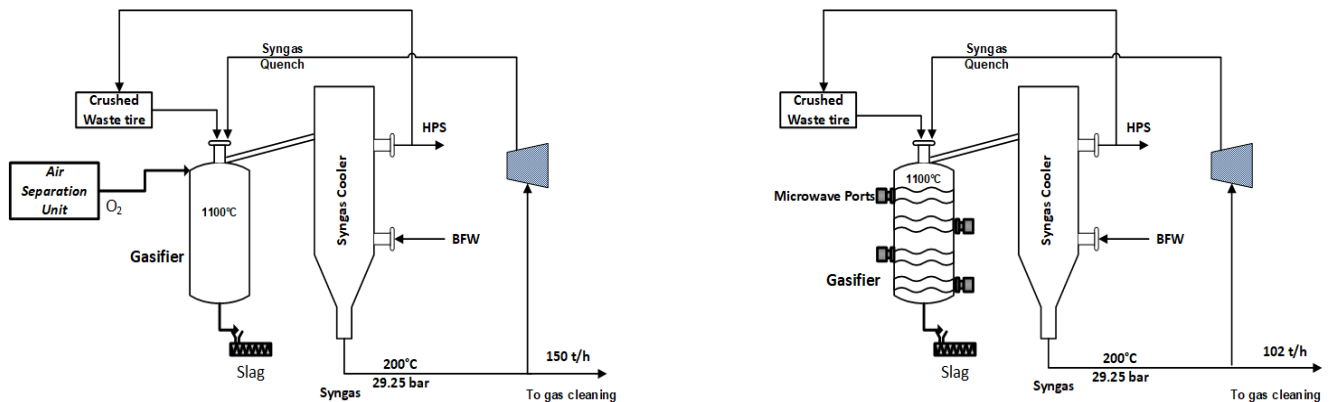

Figure 5: Gasifier design, [(A) WT-conventional process and (B) WT-electrified process] [51]

3.2.1. Sensitivity analysis for gasification temperature

The chosen operating temperature of 1100°C is determined via detailed sensitivity analysis. This analysis is focused on achieving maximum carbon conversion and minimizing the production of methane and water in the final product. The results of this analysis are visually represented in Figure 6, Figure 7 and Figure 8. The sensitivity analysis involved altering the steam-to-carbon ratios, abbreviated as S/C. As per Figure 6, when the S/C ratio is set to 8, it results in the most substantial carbon conversion. Conversely, an S/C ratio of 2 yielded the least carbon conversion. However, Figure 7 and Figure 8 depicted a contrasting pattern. Here, an S/C ratio of 8 has the

highest amounts of water, whereas an S/C ratio of 2 resulted in the lowest production of water. After considering these findings, the ideal S/C ratio is deemed to be 7, because the S/C ratio of 8 will have excess unreacted steam in the product, leading to an unnecessary increase in utility costs without corresponding benefits. At a ratio of S/C=7 and a temperature of 1100°C, carbon conversion approached near-totality (almost 100%). Simultaneously, this S/C ratio minimizing the production of methane and water in the final product.
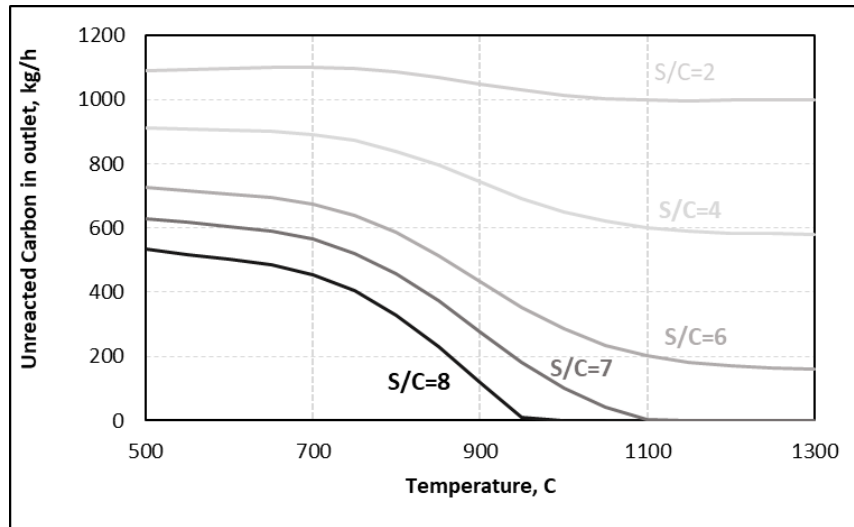
Figure 6: Carbon residue produced at various temperatures.
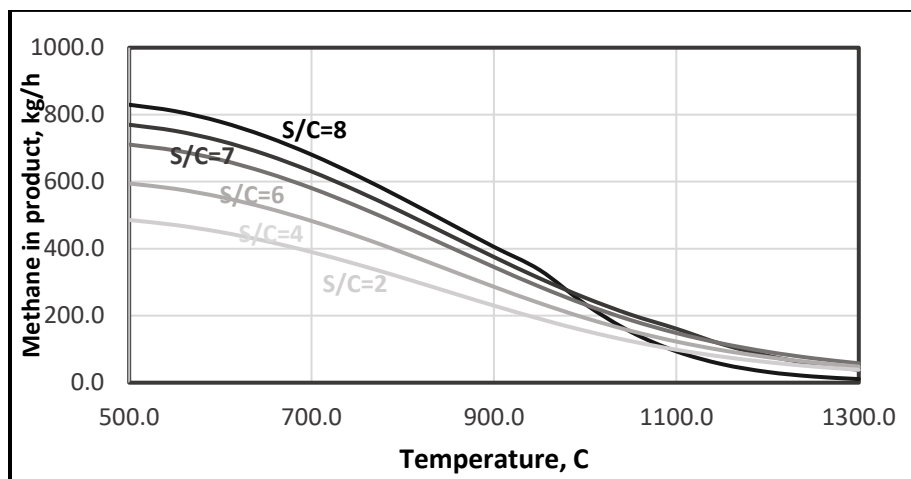
Figure 7: Methane produced at various temperatures.
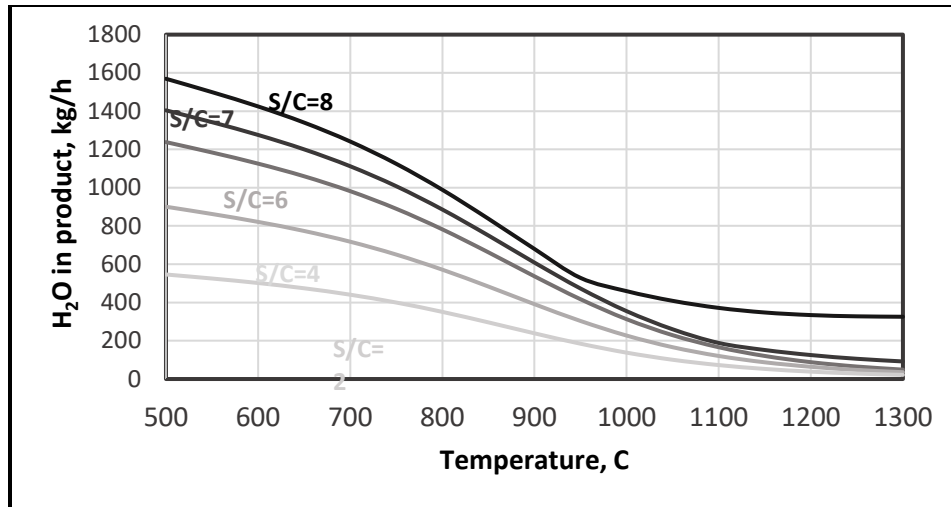
Figure 8: Moisture content in the product at various temperatures.

3.3. Gas treatment

Produced syngas is sent to the scrubber column to remove other impurities, such as dust particulates from the syngas. Both this column and the section utilized the electrolyte-NRTL model. The carbonyl sulphide (COS) hydrolysis reactor uses the syngas that exits the scrubber to turn COS into H_2S, which can be collected more effectively than COS [44]. The PFD for this unit is shown in Figure 9. In this reactor, the following reaction takes place:

$$COS + H_2O \rightarrow H_2S + CO_2$$
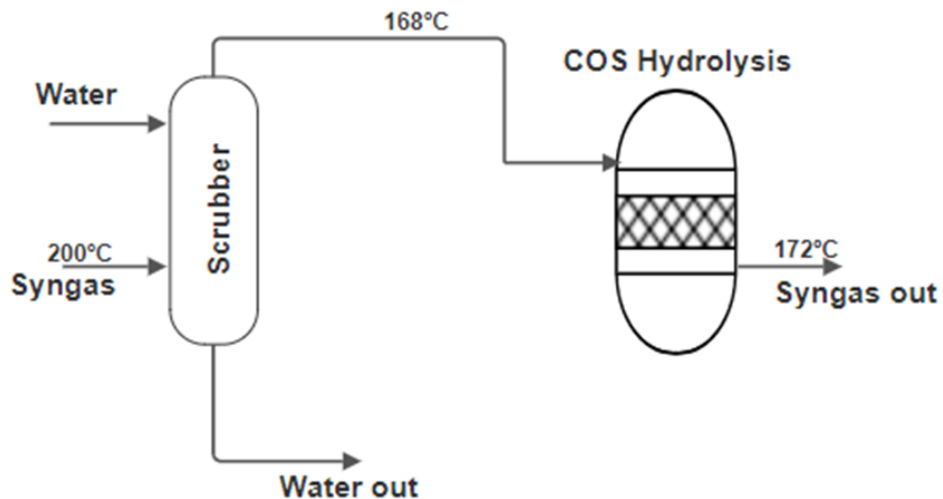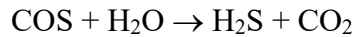
Figure 9: Process flow diagram of gas treatment unit

3.3.1. Amine unit

Research has shown that a slight presence of CO_2 in the reacting syngas can enhance methanol production [52]. On the other hand, syngas compositions without CO_2 or those with excessive CO_2 concentrations lead to poor performance [52]. A CO_2 content of 5% has been suggested as optimal [53]. In the WTC process, the CO_2 content in the syngas is more than 5%, so it is important to remove the excess CO_2 from the syngas. After COS hydrolysis, syng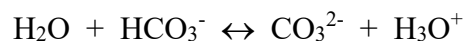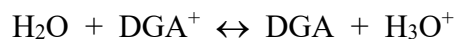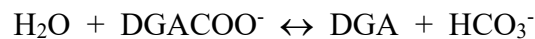as is passed through the acid gas removal unit, where DGA (Diglycolamine) is used to capture excess CO_2 and H_2S from syngas. DGA is selected due to its lower solution circulation rate, attributed to its higher solvent concentration. This leads to a greater acid gas absorption for each volume of solution circulated [54]. There are cost benefits as well because the equipment needed for DGA regeneration is smaller in size [55].

Figure 10 shows the process flow diagram of amine section. The syngas first enters the bottom of the amine absorption tower, where the gas moves in an upward direction from the bottom to the top of the absorption tower. Concurrently, the lean or regenerated amine is introduced at the top of the tower. During this process, acid components of the gas (CO_2/H_2S) are absorbed into the amine phase through a chemical reaction. The resulting amine solution, enriched with CO_2 and H_2S, exits from the bottom and is referred to as rich amine. This rich amine undergoes pumping and preheating in the stripper lean-rich heat exchanger. Subsequently, the heated rich amine is directed to the top of the stripper, where it strips out acid gases from the solution and exits the tower's top. Steam-heated reboilers at the bottom of the stripper are utilized to regenerate the rich amine, and a small amount of live steam is injected into the stripper to maintain the water balance in the system. The lean amine, regenerated from the stripper, undergoes partial cooling in the lean-to-rich solution heat exchanger before being pumped to the amine absorber, facilitated by an air-cooled exchanger. At the top of the acid gases stripping column, the gases are cooled to condense a significant portion of the water vapor. This condensed water is continuously reintroduced into the system to prevent the amine solution from becoming excessively concentrated. The reactions involved in the acid-gas removal section for absorption and regeneration of amine are shown below:

$$H_2O + DGACOO^- \leftrightarrow DGA + HCO_3^-$$

$$H_2O + DGA^+ \leftrightarrow DGA + H_3O^+$$

$$H_2O + HCO_3^- \leftrightarrow CO_3^{2-} + H_3O^+$$

$$2\ H_2O\ +\ CO_2\ \leftrightarrow\ HCO_3^-\ +\ H_3O^+$$

$$H_2O\ +\ HS^-\ \leftrightarrow\ H_3O^+\ +\ S^{2-}$$

$$H_2O\ +\ H_2S\ \leftrightarrow\ H3O+\ +\ HS^-$$

$$2\ H_2O\ \leftrightarrow\ OH^-\ +\ H_3O^+$$
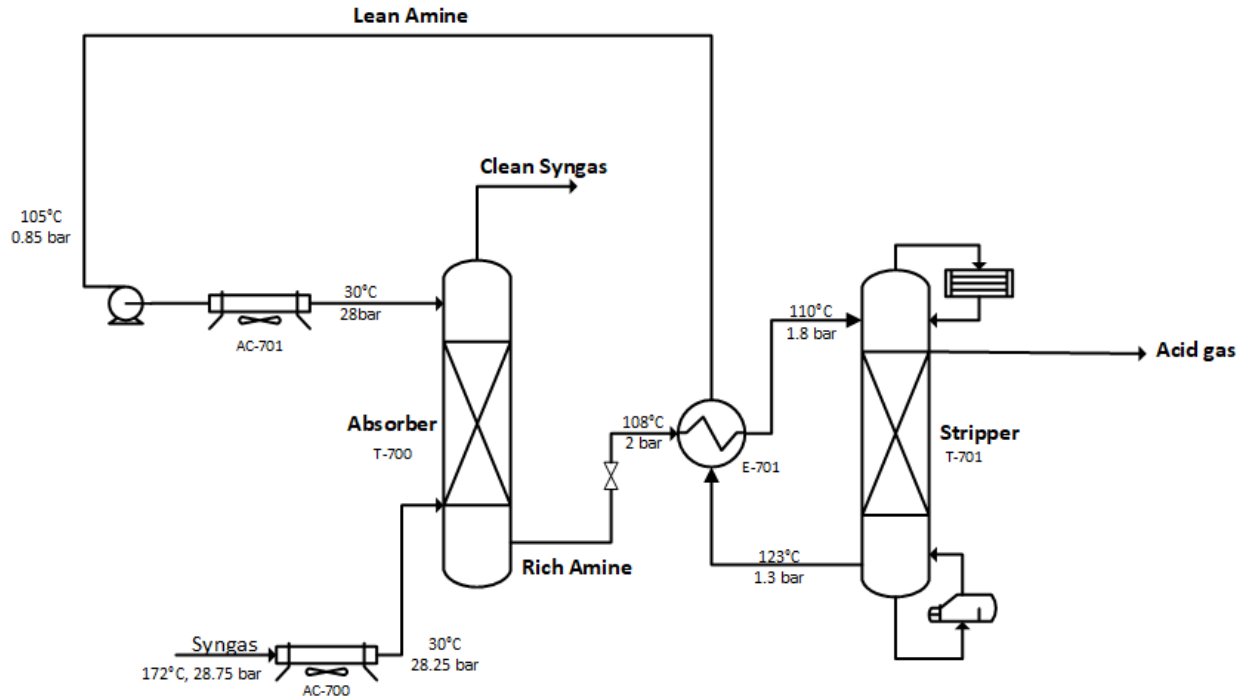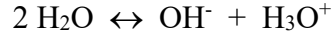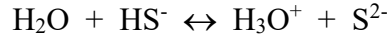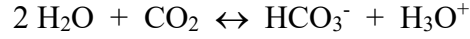
Figure 10: Process flow diagram of amine unit [56]

3.4. Methanol production

Methanol synthesis involves the utilization of a two-stage lurgi reactor system, employing a Cu/ZnO/Al$_2$O$_3$ catalyst. The reactor operates at temperatures ranging from 200°C to 300°C and pressures ranging from 50 to 100 bar, respectively. The process starts with the hydrogenation of syngas, where hydrogen is produced through the PEM electrolysis process. PEM technology was chosen because it offers several benefits compared to other electrolysis technologies, including a higher hydrogen production rate, a more compact system design, and improved energy efficiency [56,57,58]. Hydrogenation is crucial to achieve a stochiometric number (SN) equal to 2, which is necessary for methanol production [60]. If the SN exceeds 2-2.1, there will be an excess of hydrogen, leading to its accumulation in the downstream methanol loop. Conversely, a lower SN value will result in a hydrogen deficiency [61]. The equation below shows the SN formula based on the molar flow rate of CO, CO$_2$ and H$_2$.

$$SN = \frac{H_2 - CO_2}{CO + CO_2}$$
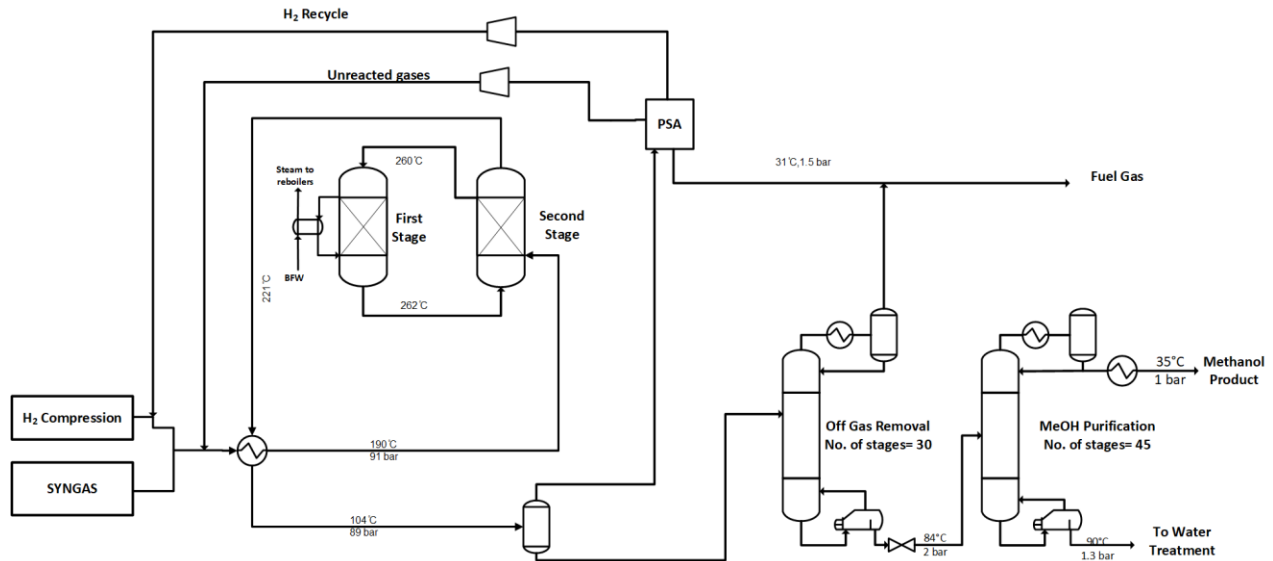
Figure 11: Process flow diagram of the methanol synthesis units [48]

The hydrogen required for the process is generated through a PEM electrolysis unit, and then it undergoes compression and water removal processes to ensure a high purity level of 99% [48]. Specifically, the Lurgi two-stage tubular reaction system is utilized for methanol synthesis. The hydrogenated syngas is directed towards a dual-stage quasi-isothermal steam-raising fixed bed Lurgi MegaMethanol reactor [62], as shown in Figure 11. This particular reactor offers improved temperature control and facilitates heat recovery with higher yields, setting it apart from alternative methanol synthesis technologies [63]. The synthesis gas is introduced into the tubes of the second reactor in a counter-current arrangement with the methanol-containing reacting gas in the reactor shell. Subsequently, the outlet synthesis gas enters the tubes of the first reactor, where the chemical reaction is initiated by the catalyst, and the remaining heat is transferred to cooling water in the shell. At this stage, a partial conversion of CO to methanol takes place. The reacting gas mixture then proceeds to the shell side of the second reactor, where its temperature is progressively reduced through the catalyst bed. The final product is extracted from a side stream of the second reactor. It's worth noting that the temperature of the first reactor is higher than that of the second reactor, resulting in the primary catalyst deactivation occurring in the first reactor. This design choice in the gas-cooled reactor ensures a practically limitless catalyst life [64]. Additionally, the control of

20

the reaction helps extend the catalyst's lifespan in the water-cooled reactor [64].

For the purification of the methanol product, a recovery section is implemented. This section consists of two separator columns, each serving a specific function. The first separator column is employed to eliminate any unreacted gases from the mixture, ensuring a more refined product. Subsequently, the second separator column is utilised to remove moisture and impurities, enabling the production of methanol with a mass purity as high as 99.85%. These steps in the overall process work in tandem to achieve the desired outcome of obtaining high-purity methanol for various applications. The steam produced in the first reactor serves to fulfill the heat demand in the distillation column's reboilers, thereby eliminating the need for external heat sources.

The kinetics for the main reactions that occur in the reactor is based on Vanden Bussche and Froment's work [53]. For brevity, all the equations and kinetics below are adapted from previous work [48]. Table 4 defines the pre-exponential constants and activation energy term values used in the following equations:

$$CO_2 + 3H_2 \leftrightarrow CH_3OH + H_2O$$
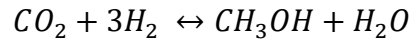
$$r_{MeOH} = \frac{k_1 P_{CO_2} P_{H_2} - k_2 P_{H_2O} P_{MeOH} P_{H_2}^{-2}}{1 + k_3 P_{H_2O} P_{H_2}^{-1} + k_4 P_{H_2}^{0.5} + k_5 P_{H_2O}} \left(\frac{mol}{kg_{cat}.s}\right)$$

$$CO + H_2O \leftrightarrow CO_2 + H_2$$
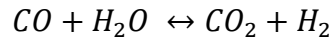
$$r_{RWGS} = \frac{k_6 P_{CO_2} - k_7 P_{H_2O} P_{CO} P_{H_2}^{-1}}{1 + k_3 P_{H_2O} P_{H_2}^{-1} + k_4 P_{H_2}^{0.5} + k_5 P_{H_2O}} \left(\frac{mol}{kg_{cat}.s}\right)$$

Table 4: Kinetic values of the MeOH synthesis reactions

Reaction constant $\left(\ln k_i = A_i + \frac{B_i}{T}\right)$	A_i	=Bi (k)
k_1	-29.87	4811.16
k_2	17.55	-2249.8
k_3	8.15	0.00
k_4	-6.45	2068.44

k_5	-23.44	14928.92
k_6	4.80	-11797.45
k_7	0.13	-7023.5

3.5. Simulation results

Table 5 presents a summary of the process simulation results for each methanol production pathway. The design basis for both the electrified and conventional pathways is based on a waste tire feed rate of 50 tonnes/h. Table 5 shows that the conventional pathway yielded a methanol production rate of 79 tonnes/h, with direct CO_2 emissions of 31.4 tonnes/h. On the other hand, the electrified pathway produces 93 tonnes/h of methanol, along with CO_2 emissions of 13.7 tonnes/h. Additionally, both processes utilize the flue gas generated during methanol production to generate electricity. The electrified pathway generates 29.9 MW of electricity, while the conventional pathway produces 15.3 MW. These findings highlight the contrasting performance of the two pathways in terms of methanol output and associated CO_2 emissions.

Table 5: Simulation results

	WT – Electrified	WT - Conventional
Input, tonne/h		
Waste tires	50	50
Total electricity demand, MW	477.9	351.8
Product output, tonne/h		
Methanol	93	79
Oxygen	35.2	-
Electricity, MW	29.9	15.3
Emissions, tonne/h		
CO_2	12.7	31.4
NO_2	4.0E-4	4.51E-5
NO	2.28E-4	1.8E-4

SO$_2$	1.71E-6	2.11E-5
CH$_4$	-	9.15E-5
H$_2$S	3.35E-41	3.15E-4

3.6. Life cycle assessment (LCA)

LCA is performed according to the ISO 14040 standard, which outlines the four phases of the assessment: Goal and scope definition, life cycle inventory analysis, life cycle impact assessment and results interpretation. LCA framework is shown in Figure 12.
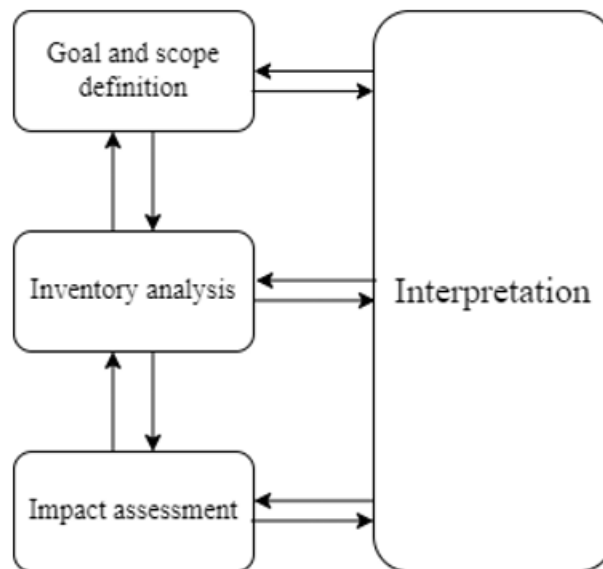
Figure 12: LCA framework according to ISO 14040 [65]

3.6.1. Goal and scope definition

The goal of this study is to evaluate the environmental effects of producing methanol through end-of-life tire recycling, comparing a novel WTE process with traditional approaches like WTC, as well as with methanol production from natural gas and coal. The assessment considers different electricity sources for powering the process. The main focus of this study lies in conducting a Life Cycle Assessment (LCA) to gauge environmental impacts, primarily related to greenhouse gas emissions (GHG), stemming from the process. The environmental impacts observed will be benchmarked against the emissions from NG to methanol process, which serves as the base case

for this analysis. This is a cradle-to-gate analysis where the end gate is the commercial scale methanol production for the market. However, aspects such as emissions for the production of tires, plant construction, equipment maintenance, product distribution, use, and end-of-life treatments are excluded from this study. Unlike other studies, no credit has been considered for the use of waste tires. The study is concentrated solely on emissions occurring during the production process. The system's boundaries for the LCA, as depicted in Figure 13, encompass waste tire processing, methanol production, and electricity consumption.
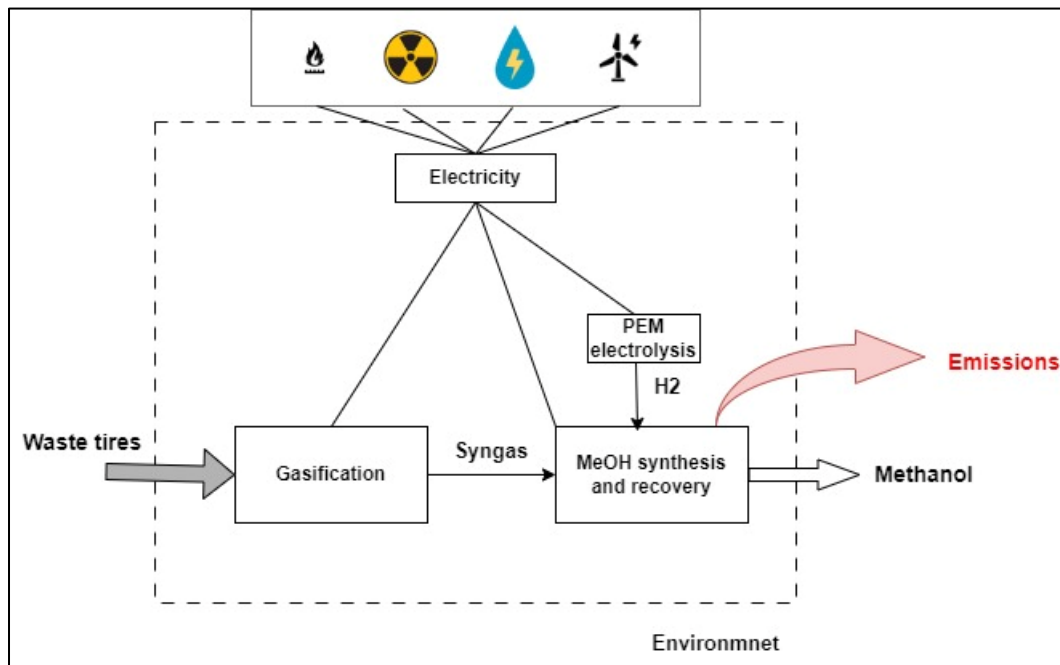
Figure 13: System boundary for LCA study

3.6.2. Life cycle inventory analysis

The inputs and outputs of product systems are derived from simulation results obtained through Aspen Plus for both WT-electrified and WT-conventional processes. The input and output data based on simulation results presented in Table 5, is used for the LCA analysis. When conducting the LCA for these processes, it is important to consider the carbon intensity and other environmental implications associated with power generation. The emissions from electricity generation vary with different electricity generation sources. To account for this diversity, the study considered different renewable and non-renewable sources: Natural gas, Nuclear, Hydro and

Wind. The location of the pilot plant is selected to be in Canada. In Canada, different provinces uses a variety of electricity sources resulting in different emissions in each province, for diversity factor this study will asses the CO_2 emissions in three different provinces: Quebec, Ontario and Alberta, according to their energy profiles [66]. The GHG emissions by different grids in Quebec, Ontario and Alberta are shown in Table 6. The LCA data for these electricity production sources nad emissions data for NG-methanol were obtained from the Ecoinvent database and CRAIG report [67] and assessed using OpenLCA software v1.11.0. For a better understanding, the functional unit for LCA calculations is taken as one kilogram of methanol product for both processes.

Table 6: GHG emission per kWh pf electricity generated in three different provinces [67]

Province	Quebec	Ontario	Alberta
g CO₂ eq./kwh	17.7	39.3	682.8

3.6.3. Life cycle impact assessment (LCIA)

A comprehensive evaluation of different impact categories is performed using the TRACI 2.1 method for mid-point analysis and the ReCiPe End-point (H,A) method for end-point analysis. The TRACI 2.1 is a widely used method for LCA purposes, mainly in North America, employed to quantify ten impact categories [68]. The ReCiPe End-point impact assessment method is an upgraded method that combines both Eco-indicator 99 and CML method [68]. This method provides an estimation of the impacts in terms of damage points per kilogram of product. It primarily encompasses three main categories or end-points: ecosystem quality, human health, and resources. These end-points comprise numerous subcategories, allowing for a detailed assessment of the overall impacts. The flow diagram of impact categories included in midpoint and endpoint assessment is shown in Figure 14.
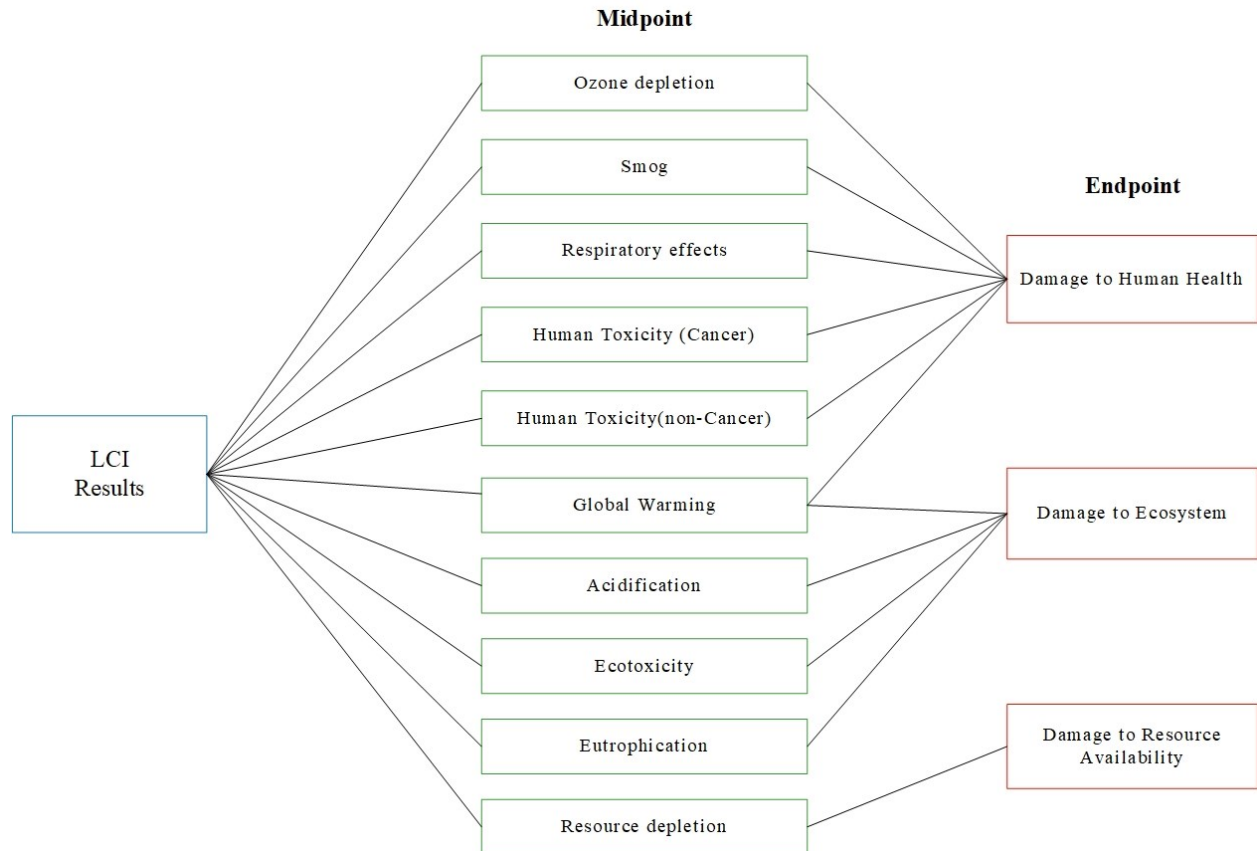
Figure 14: Flow diagram of midpoint and endpoint impact categories [69]

Chapter 4: Results and Process Economics

4. Results

4.1. Electricity demand

The variation in electricity demand between WT-electrified and conventional processes is due to the different heat supply methods used in both processes. The WT-electrified process uses a microwave heating gasifier. In contrast, the WT-conventional uses a thermal gasifier that partially combusts the inlet feed to supply the heat demand of the gasification reactions. As a result, the overall electricity for WT-electrified is higher than that of the conventional process. In the electrified process, the waste tire conversion into methanol requires 4.83 kWh of electricity per kilogram of MeOH. Whereas, conventional process requires 4.17 kWh of electricity per kg of MeOH. A more detailed analysis of electricity demand is shown in Figure 15 for different process units in both pathways. Total electricity demand in the WTE and WTC process is 477.9 MW and 351.8 MW, respectively. Overall, the PEM electrolyser for H_2 production consumes the highest electricity compared to other units. In the H_2 unit, 90% of total electricity is consumed in the conventional process, whereas 53.5% of total electricity is consumed in the electrified process because the syngas from WTE process require lower hydrogen than the conventional process.

Figure 15: Electricity demand for WT-electrified and conventional process

4.2. Energy efficiency

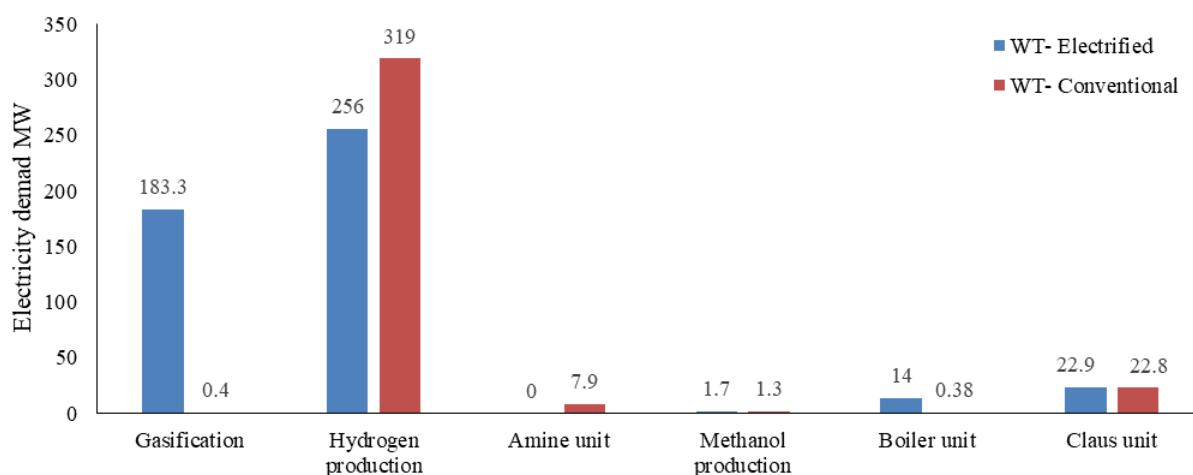The energy efficiency of a process is an important factor in determining its energy conversion performance. The WT-electrified process exhibited an energy efficiency of 55.8%, while the WT-conventional process achieved a slightly lower energy efficiency of 54.6%. These values indicate the proportion of input energy that is successfully converted into useful output energy within each respective process. The enhanced efficiency of the WT-electrified process can be attributed to its ability to yield a higher product output from an equivalent amount of feed compared to the conventional method.

$$Thermal\ efficiency = \frac{Energy\ of\ the\ methanol\ product(MW, LHV)}{Energy\ of\ waste\ tires\ (MW, LHV) + Net\ electricity\ demand(MW)}$$

4.3. LCA Results

4.3.1. LCA of electricity generation

As discussed, electricity plays a significant role in the lifecycle GHG emissions of each pathway. Therefore, it is essential to consider clean electricity to reduce the proposed process's carbon footprint. Table 7 shows the LCA results for 1 kWh of electricity generated by different sources. Results were taken from the Ecoinvent database (v3.8). Data is collected from different electricity generation sources in Canada, i.e., Natural gas plant in Alberta, Nuclear power plant in Ontario, and a hydroelectricity and wind power plant in Quebec. For reference the datset selected from ecoinvent for the calculation of this analysis is shown in the appendix.

Table 7: LCA results of different electricity sources (per kWh)

Parameter	Unit	Natural Gas	Nuclear	Hydro	Wind
Acidification	kg SO_2 eq	2.2E-4	1.1E-4	2.69E-5	4.46E-05
Eutrophication	kg N eq	4.22E-05	1.1E-4	1.2E-5	4.49E-05
Fossil fuel depletion	MJ surplus	1.26	0.016	0.0028	0.018
Global warming	kg CO_2 eq	0.426	0.013	0.0048	0.01

Ozone depletion	kg CFC-11 eq	2.29E-08	1.48E-09	2.87E-10	6.35E-10
Respiratory effects	kg PM2.5 eq	1.80E-05	3.41E-05	3.67E-6	1.40E-05

The system boundary for the LCA primarily encompasses four stages: the upstream phase, transportation and construction phase, operation and maintenance phase, and decommissioning phase [70]. Table 7 shows that electricity from natural gas has the highest emissions in each parameter per kWh of electricity except for the eutrophication nad respiratory effects because it accounts for the highest fossil fuel consumption, leading to more CO_2 and other emissions. In contrast, electricity from hydro and wind has the lowest emissions as they are renewable sources. Studies showed that wind power has comparatively higher environmental impacts, mainly due to the upstream and decommissioning stages [70]. In comparison, hydropower and nuclear life cycle had lower environmental impacts. Thus, fossil depletions are higher for wind compared to nuclear. Emissions related to hydropower are mainly due to construction and operations related to dams and reservoirs [71]. Hydropower from reservoir and non-alpine based powerplants showed the highest environmental impacts due to the construction and transportation challenges arising from the limited availability of materials in those regions.

4.3.2. Process life cycle emissions

TRACI 2.1 midpoint analysis results for WTE and WTC processes with four different electricity sources are shown in Figure 16, Figure 17, Figure 18, and Figure 19. The WTE process demonstrates lower global warming emissions across all energy sources compared to the WTC process. The emissions are especially minimal when Nuclear, Hydro, or Wind power is employed. The parameters like Ozone Depletion, Acidification, Eutrophication, and Respiratory Effects, each measured in their specific units, generally exhibit a similar pattern - WTE has lower values than WTC across all energy sources. However, an exception is observed when it comes to hydropower. In this case, the WTE process results in higher emissions. This is because these parameters are significantly influenced by the electricity generating source, and since the WTE process has a higher electricity demand, it consequently leads to greater emissions. This trend is also mirrored

in the Fossil Fuel Depletion parameter. Here, the WTE process registers higher values across all energy sources, reflecting its greater electricity demand compared to the WTC process.
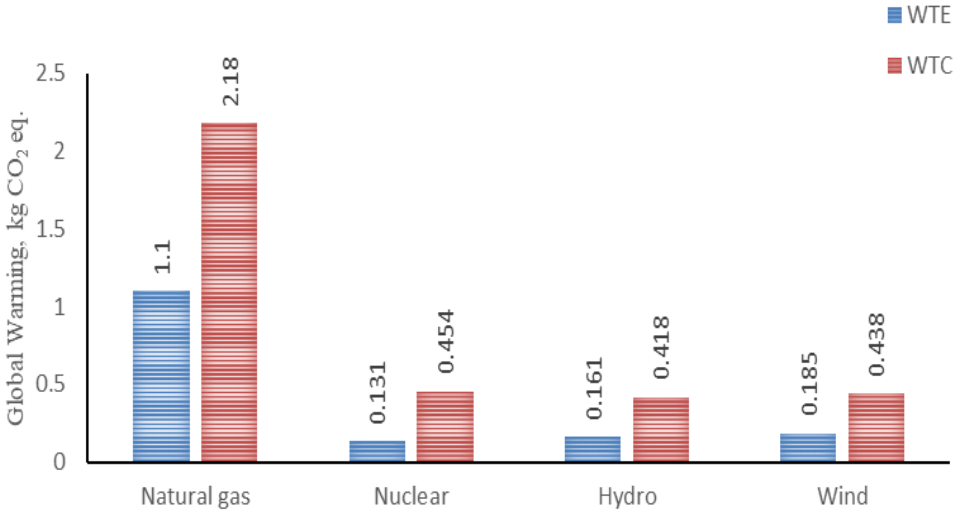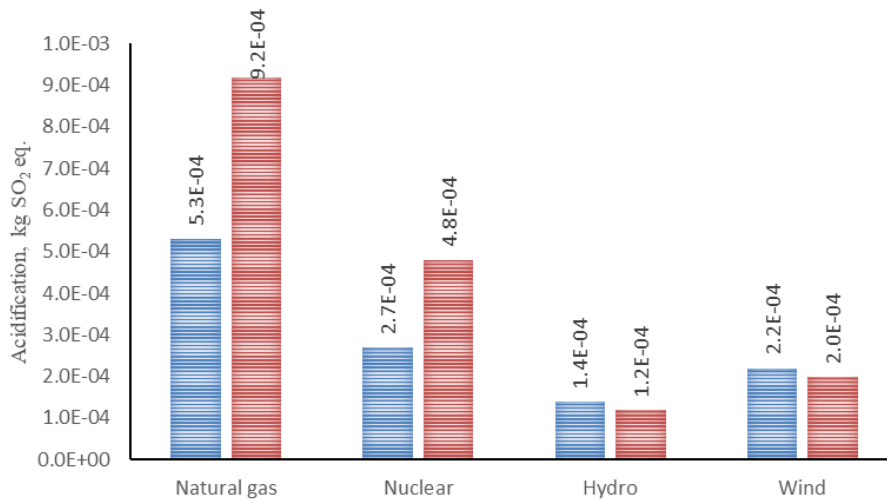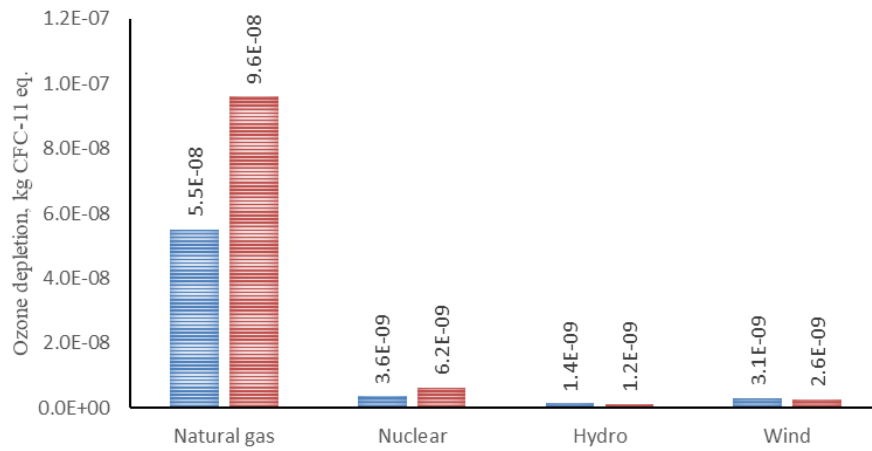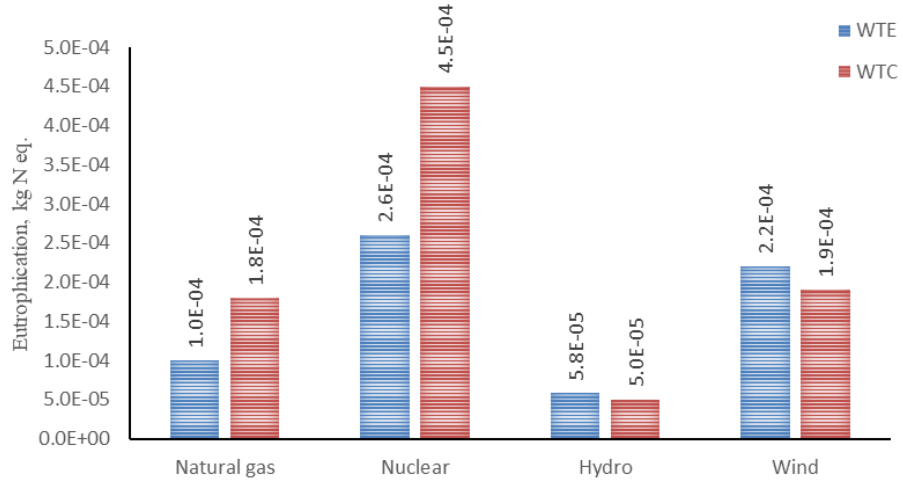

Figure 16: TRACI 2.1 results for global warming

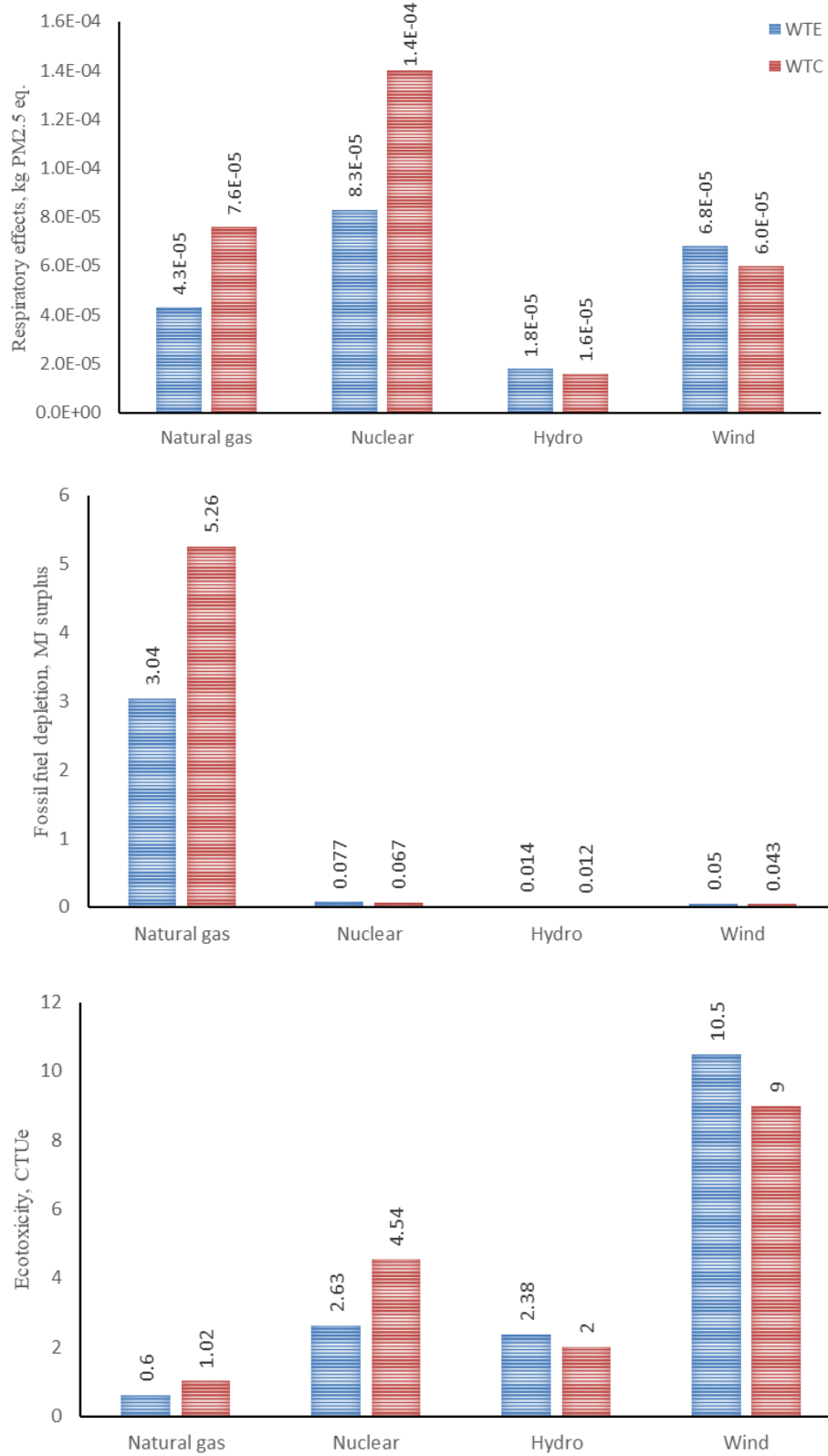Figure 17: TRACI 2.1 results for eutrophication, ozone depletion and acidification

Figure 18: TRACI 2.1 results for respiratory effects, fossil fuel depletion and ecotoxicity
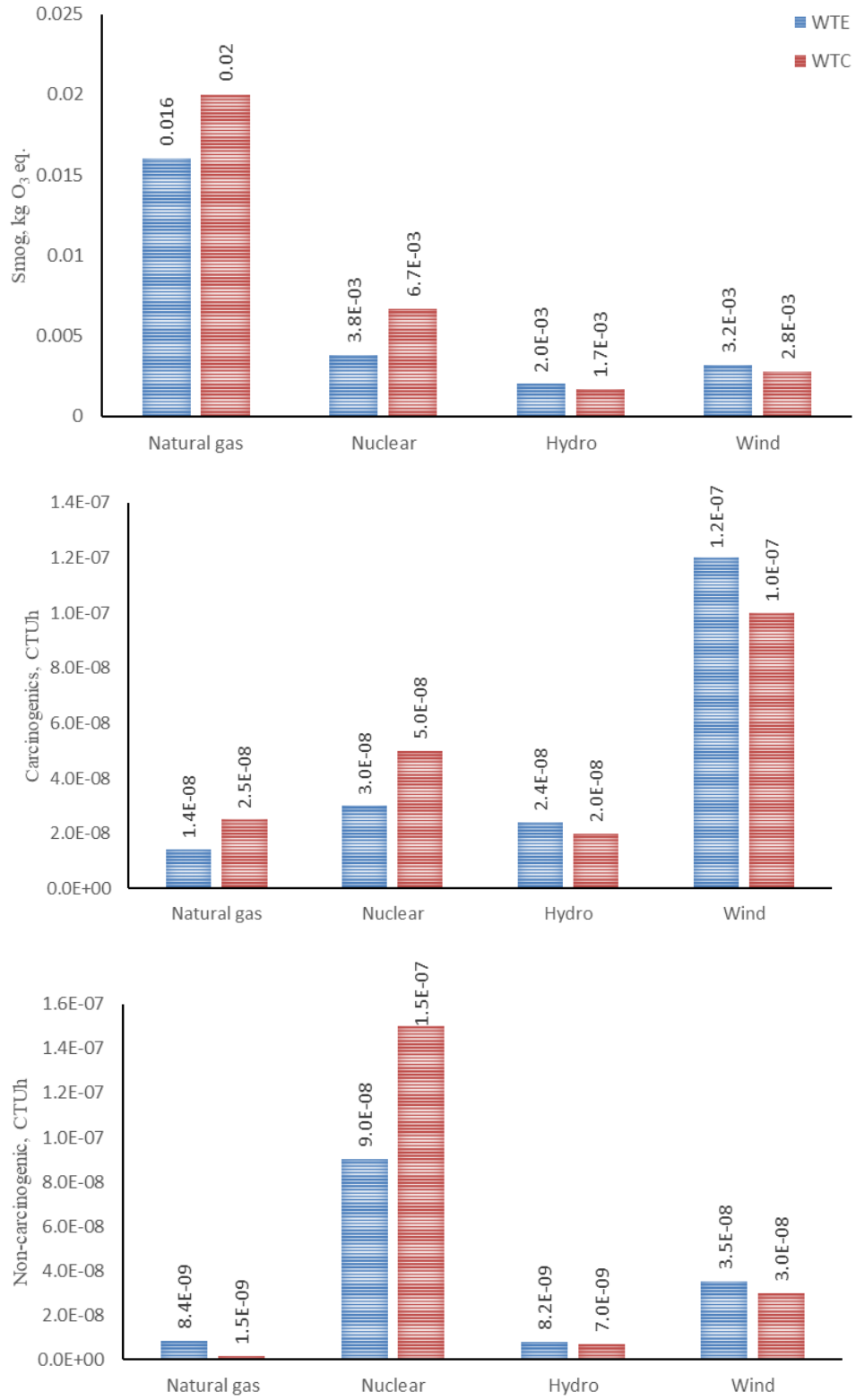
Figure 19: TRACI 2.1 results for smog, carcinogenic and non-carcinogenic

Figure 20 shows the GHG emissions associated with the WTE and WTC processes when powered by electricity from three Canadian provinces: Quebec, Ontario, and Alberta. Notably, Quebec records the lowest emissions among the other three provinces for both processes. WTE process has the lowest emissions in Quebec, with Ontario coming in second. However, when Alberta's electricity is used, WTE has higher emissions than WTC. This pronounced difference in Alberta's GHG emissions can be attributed to its energy mix. A substantial 91% of Alberta's electricity is derived from carbon-intensive sources such as coal, coke, and natural gas [66]. In contrast, Ontario's electricity generation relies on fossil-based fuels for only 7% of its output [66]. Most notably, Quebec stands out with less than 1% of its electricity generation hinging on fossil fuels while the rest from renewable sources [66]. The data underscores the profound influence of energy sourcing choices on regional GHG emission profiles.
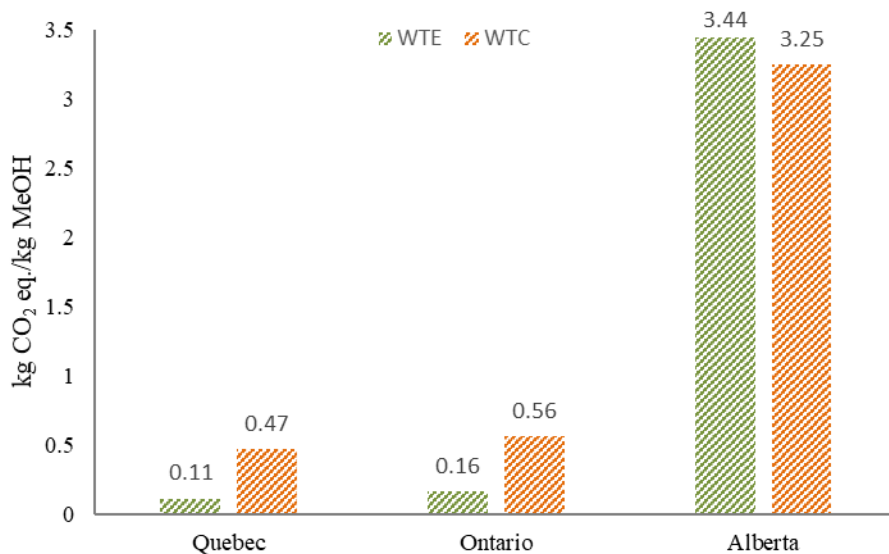
Figure 20: GHG emission of WTE and WTC in three different provinces

Globally, about 55-65% of methanol is produced from natural gas, and about 30-35% is produced from coal [72]. So, it is important to know how much WTE performs better in terms of GHG emissions than other conventional methods. Figure 21 presents the GHG emissions for four distinct processes: WT-electric, WT-conventional, natural gas to methanol, and coal to methanol. Coal to Methanol has the most significant GHG emissions, discharging 2.5 kg of CO_2 (GREET v1.3.0) per kilogram of methanol produced. The high carbon content in coal and the intensive energy required for this process results in high GHG emissions. Whereas the Natural Gas to Methanol

method yields lower GHG emissions than coal to methanol, with an emission rate of 1.02 kg of CO_2 equivalent (Ecoinvent v3.8) per kilogram of methanol. The procedure involves converting methane, the main component of natural gas, into methanol. Although this process is more efficient and less carbon-intensive than the coal to methanol conversion, it still contributes to GHG emissions. WT-electric and WT-conventional show the lowest GHG emissions compared to fossil-based conventional pathways. In which WT-electrified depicts the lowest emissions compared to all, i.e. 0.16 kg CO_2 eq. per kg of methanol when hydro-based electricity is used for power demand. In summary, Figure 21 illustrates the significant differences in GHG emissions from these four processes, highlighting the environmental advantages of WT-electric over WTC and traditional fossil fuel-based processes.
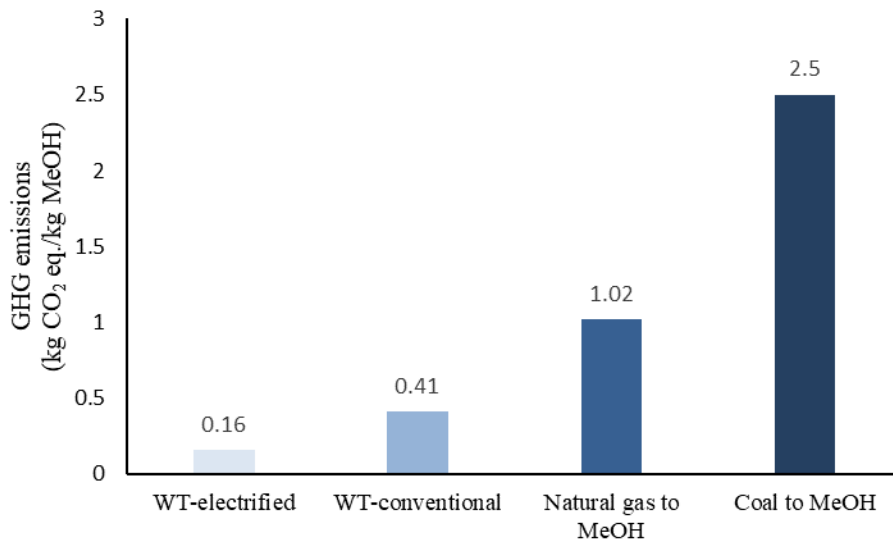
Figure 21: GHG emissions WTE compared with other technologies

Figure 22 and Figure 23 shows the ReCiPe end-point results of the WT-electrified and WT-conventional process, respectively. These results have been normalized with end-point results of Natural gas to methanol process as baseline. On comparing WTE and WTC processes, it can be seen that the WTE process has the lowest damage points with each electricity generation source. Figure 22 demonstrates that the WTE process with hydroelectricity has the lowest damage point in all three categories. Using electricity from natural gas has the highest damage points, followed by nuclear and wind. A similar trend can be seen in Figure 23; the WT-conventional process performs better with hydroelectricity and wind. Natural gas accounts for the highest damage points

in all three categories because it is responsible for the highest resource depletion, results in more emissions which affect both ecosystem quality and human health.
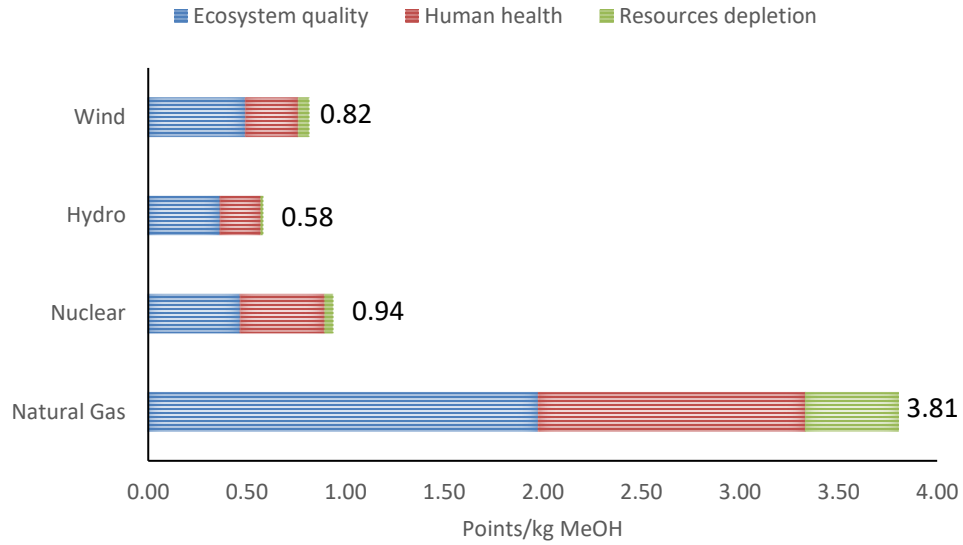
Figure 22: End-point results for WT-electrified
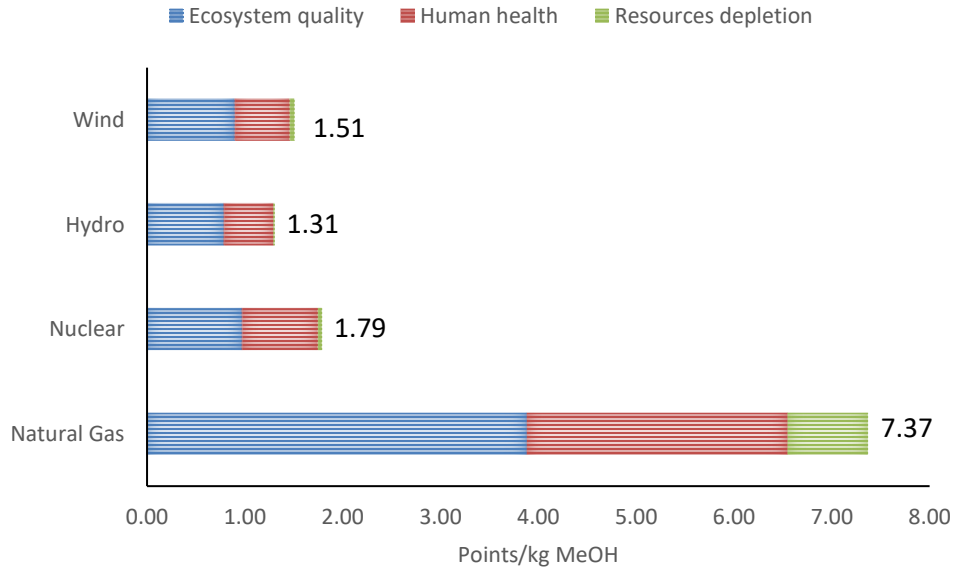
Figure 23: End-point results for WT-conventional

4.4. Economic analysis

Table 8 shows the economic assumptions and parameters used for the economic analysis of WTE and WTC processes. The economic evaluation is estimated for 2022 year, and the currency used here is US Dollars. All economic analysis parameters, utility prices, market prices, and assumptions used to calculate the NPV are listed in Table 8. Notably, the utility and market prices presented reflect only the "base-case" calculations and a sensitivity analysis is discussed to account for potential price changes in a further section. Financial parameters, such as interest rates, were based on prior recommendations.

Table 8: Base case market price and economic assumptions

Feed and product prices	
Electricity, USD/kWh	0.04 [73]
MeOH price, USD/tonne	585 [74]
Economic assumptions [75]	
Operation time (hr/year)	8760
Capacity factor	90%
Chemical engineering plant cost index	814.6 [76]
Plant lifetime (year)	30
Loan lifetime (year)	15
Interest rate on loan	5%
Debt percentage	40%
Inflation	3%
Federal + provincial tax rate	26%
Internal return rate	10%

4.4.1. CAPEX

The profitability of each process is assessed by analysing the net present value (NPV), which serves as the primary economic indicator. Capital costs were determined from various sources, including published data wherever possible, such as the gasification section, PEM electrolysis, MeOH synthesis unit, and amine unit. For all other units, the Aspen cost estimator software is utilised to estimate the capital costs of individual unit operations, such as pumps, compressors, and distillation columns. The equipment cost is calculated based on its size and the estimation year outlined in their respective reference. The cost is calculated using the formula given below,

$$\text{Equipment cost} = Cost_{Ref} \times \left(\frac{Capacity}{Capacity_{Ref}}\right)^n \times \left(\frac{CEPCI}{CEPCI_{Ref}}\right)$$

where n denotes the capacity factor ranging from 0.6 to 1, depending on the equipment. After determining the equipment cost, the total capital investment cost can be calculated using the parameters shown in Table 9. Moreover, the annualised CAPEX is calculated by multiplying CAPEX with the annualisation factor (AF). The AF is calculated using the formula shown below,

$$AF = \frac{i(1+i)^N}{(1+i)^N - 1}$$

where i denoted the interest rate, and N shows number of years.

Table 9: Capital investment cost estimation parameters [77, 78]

Cost Parameter	Value
Delivery Cost	8% of equipment cost
Direct Cost (% of Delivered cost)	
Installation Cost	
Equipment Erection	40%
Piping	70%
Instrumentation	20%
Electrical	10%
Utility Cost	10%
Off-sites	20%
Buildings	20%
Site Preparation	10%
Land	6%
Indirect Cost (% of Total Direct Cost)	
Engineering and Supervision	22%
Construction Overhead	18%
Project Contingency	10% of fixed capital investment
Fixed Capital Investment (FCI) = Direct Costs + Indirect Costs	
Startup Costs	9% of fixed capital investment
Working Capital	15% of total capital investment
Total Capital Investment (TCI) = Fixed Capital Investment + Startup Costs + Working Capital	

4.4.3 OPEX

The operating cost of a plant refers to the ongoing expenses incurred in running and maintaining its operations. It encompasses various elements such as the costs of raw materials, utilities like electricity, labor wages, equipment maintenance, facility overhead expenses, insurance, taxes, and general day-to-day operational costs. Understanding and managing these operating costs is essential for businesses to assess the financial efficiency and sustainability of their industrial operations. By controlling and optimizing these expenditures, companies can enhance profitability and make informed decisions about resource allocation and process improvements. The calculation of labor wages takes into account various factors, including the size of the plant, the prevailing wage rate for labor, the number of work shifts, and the total count of operators assigned to each shift, for this equation given in Perry's Chemical Engineering Handbook [79] is used. Labor wages are based on the estimation year of 2022. All the parameters used for the OPEX calculation are shown in the Table 10.

Table 10: Operating cost estimation parameters [79, 80]

Cost Parameter	Value	
Supervision & Engineering	22%	of Labor Wages
Operating Supplies & Services	6%	of Labor Wages
Laboratory Expenses	15%	of Labor Wages
Payroll Charges	35%	of Labor Wages + Supervision & Engineering
Maintenance Costs		
Maintenance Wages	4.5%	of FCI (Excluding Land)
Maintenance Supervision & Engineering	25%	of Maintenance Wages
Material Supplies	100%	of Maintenance Wages
Maintenance Overhead	5%	of Maintenance Wages
Overhead Costs		
Plant Overhead	7.1%	of TWSE*
Mechanical Department Services	2.4%	of TWSE*
Employee Relations Department	5.9%	of TWSE*
Business Services	7.4%	of TWSE*
Property Insurance & Taxes	2%	of fixed capital investment
General Expenses		
Sale Expenses	3%	of Sales
Research & Development	5%	of Sales
Administrative Expenses	3%	of Sales

*TWSE is the total operating and maintenance wages, supervision, and engineering expenses

Table 11 outlines the financial comparisons between the WT-electrified and WT-conventional processes in terms of equipment cost, annualised CAPEX, operating costs, and the minimum selling price (MSP) of methanol. The MSP indicates the price at which methanol must be sold to achieve a Net Present Value (NPV) of zero for the plant.

For the equipment costs, the WTC process incurs a higher gasification unit cost because its syngas flowrate exceeds that of the WTE process by 48 tonnes/h. Conversely, the syngas cleaning section is more expensive in the WTE process, as it handles a 16 tonne/h greater syngas flowrate than the WTC process. This is largely attributed to the WTC process removing most of its CO_2 in its amine unit. Furthermore, the WTC process has a more expensive hydrogen production due to its higher demand. On the other hand, the methanol production cost in the WTE process is elevated because it produces 14 tonnes/h more methanol than the WTC process. Notably, the electricity generation in the WTE process is almost double that of the WTC, leading to a higher associated cost.

From Table 11, it's clear that the WTC process's capital cost exceeds the WTE process. This is primarily attributed to the conventional process incorporating an additional amine unit. The overall capital investment for the WTC process stands at 161 million dollars, compared to the 145 million dollars needed for the WTE process. Despite the conventional process's higher upfront costs, its operational expenses are less than the electrified process due to the latter's increased production rates. Specifically, the WTE process's operating cost is $351 million, while the WTC process comes in at $330 million. Also, the methanol's selling price from the conventional process is $157/tonne more than that of the electrified process. This discrepancy primarily stems from the lower capital costs and improved efficiency of the electrified approach.

Table 11: Economic analysis summary of electrified and conventional pathways

	WT-electrified	WT-conventional
Direct capital cost, $Million		
Gasification [45]	227.6	228.0
Microwave heating technology [81]	6.9	-
Amine unit [45]	-	98.6
Syngas Cleaning [45]	27.6	25.6
H_2 production and compression [45]	171	219
MeOH synthesis and purification [44]	97.6	90.5

Power generation	40	8.75
Air separation unit (ASU) [44]	-	0.06
Clauspol unit [45]	12.3	-
CAPEX and OPEX at 90% of design capacity, $Million/year		
Annualised CAPEX	145	161
OPEX	402	369
Sale at 90% of design capacity, $Million/year		
Methanol sale	524	527
Oxygen sale	20	-
Total revenue, $Million	544	527
Minimum selling price of methanol, USD/tonne	795	940

4.3.1. Sensitivity analysis- MSP at different electricity prices

A sensitivity analysis is conducted on WT-electrified and WT-conventional processes to examine the impact of varying electricity prices on methanol's minimum selling price (MSP). From Figure 24, it can be observed that MSP increases linearly with an increase in electricity prices. The study analyzed the MSP in two Canadian provinces, Quebec, with the lowest electricity price, and Alberta, with the highest electricity price. In Quebec, where the electricity price is $0.04/kWh [73], the MSP is the lowest at $795. Alberta, with a higher electricity price of $0.1/kWh [73], corresponded to an MSP of $1120. When compared to the conventional process, which had an MSP of $940 and $1230 with the same electricity price as in Quebec and Alberta, respectively. These findings underscore the significant impact of local electricity costs on the economic viability of methanol production. Therefore, any strategies aimed at optimizing methanol production should consider the local energy landscape.
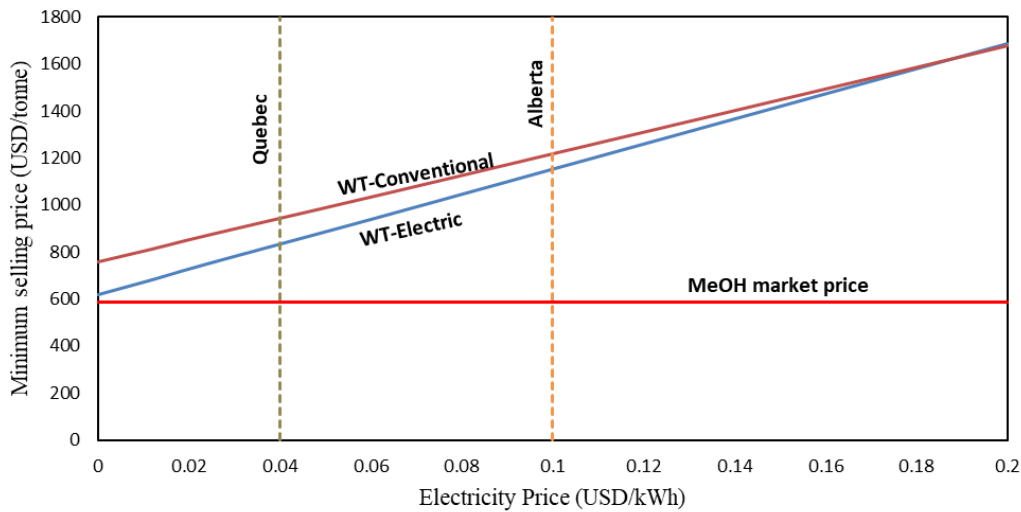
Figure 24: Effect on minimum selling price at different electricity prices

4.3.2. Sensitivity analysis- MSP at different CAPEX of electric gasifier

The cost of the gasifier significantly impacts the total capital investment in both the WT-electrified and WT-conventional processes. The WT-electrified process employs a gasifier that operates on microwave heating. However, due to the lack of commercial cost data for microwave reactors, it's crucial to analyse how fluctuations in the reactor price might influence the MSP of methanol. In this study, a sensitivity analysis is conducted using three scenarios: the base case, half of the base case reactor price, and twice the base case reactor price. The base case is defined with the reactor price at $156 million [40], with an additional $7 million [81] attributed to microwave heating technology. Figure 25 illustrates the sensitivity analysis results for these three scenarios and the effects of varying electricity prices on the MSP. For example, Quebec, which has the lowest electricity rates, shows an MSP of roughly $687/t when the reactor price is halved and an MSP of $1000/t when the reactor price is doubled. In contrast, Alberta, with the highest electricity rates, sees an MSP of $1013/t when the reactor price is reduced by half and over $1330/t when the reactor price is doubled. The results yield an interesting observation: there is only a slight difference in the MSP between the base case and when the reactor price is reduced by 50%. However, a substantial increase in the MSP is noted when the reactor price doubles, underscoring the significant influence of the reactor price on the MSP of methanol.
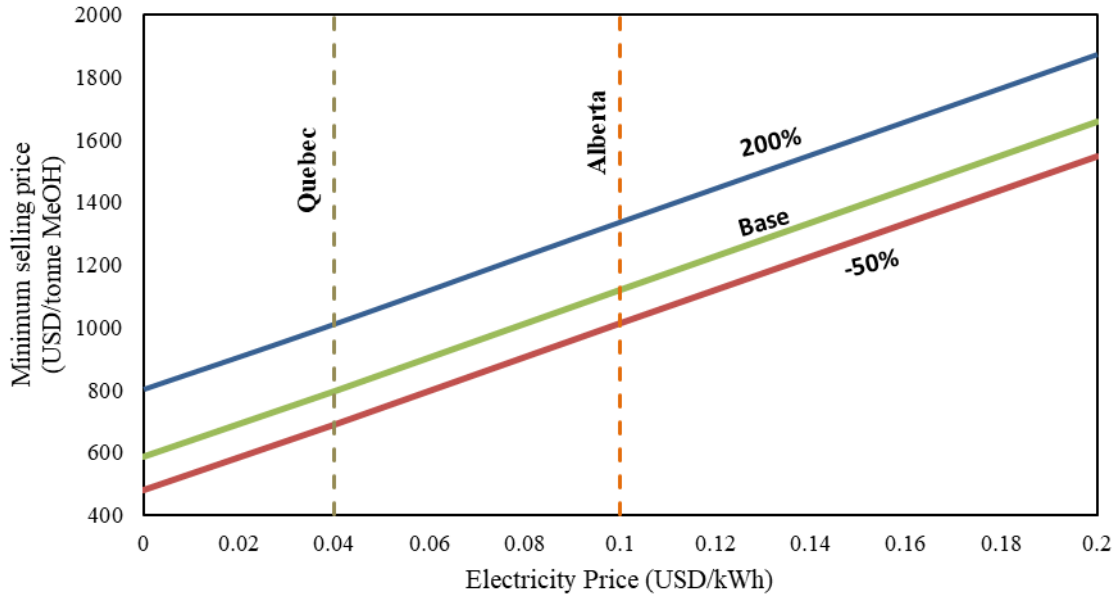
Figure 25: Effect on minimum selling of MeOH at different CAPEX of electric gasifier

4.3.3. Avoided GHG credit

One of the key parameters to analyse is the required GHG credit for the electrified and conventional processes to reduce their MSP and make them competitive with the current market selling price of methanol. The formula for calculating GHG credit is shown below. The baseline for this calculation is the GHG emissions and current market price of methanol from conventional process. For the conventional NG process, GHG emissions is 1020 kg eq. CO_2/ tonne of MeOH, which is calculated from the NG to methanol and the current market price for methanol is $585/tonne.

$$Avoided\ GHG\ credit = \left\{\frac{MSP_{WT} - MSP_{NG}}{GHG_{NG} - GHG_{WT}}\right\}$$

Where,

MSP_{WT} : MeOH min. selling price of waste tire process (USD/t MeOH)

MSP_{NG} : MeOH min. selling price of NG-MeOH process (USD/t MeOH)

GHG_{WT} : GHG emissions from waste tire process (t CO_2 eq/t MeOH)

GHG_{NG} : GHG emissions from NG-MeOH process (t CO_2 eq/t MeOH)

43

Based on the data in Figure 26, it can be observed that the electrified process generally demands lower GHG credits compared to the conventional process, especially when renewable electricity is utilised. For instance, when the electricity emits 50 tonnes of CO_2 per MWh, the electrified process only needs a GHG credit of $329 per tonne of CO_2, whereas the conventional process requires a credit of $862 per tonne CO_2. This showcases a significant difference between the two approaches. Moreover, as the carbon intensity increases to 100 tonnes of CO_2 per MWh, the required credit for the electrified process is $528 per tonne of CO_2. In contrast, the conventional process necessitates a credit that is more than three times, i.e. $1740 per tonne of CO_2. Therefore, this data highlights that opting for an electrified process, especially one powered by renewable electricity, can result in a lower demand for GHG credits compared to the conventional process. This suggests that the electrified process is generally more beneficial in terms of GHG emissions and credit required to reduce the methanol selling price, making it competitive with the market price.
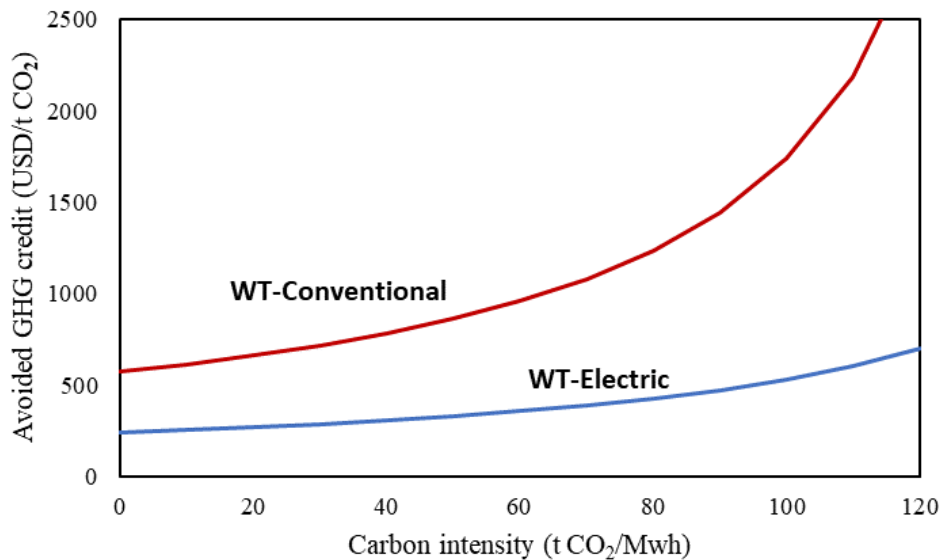

Figure 26: Avoided GHG credit required for different carbon intensity

Conclusion

This research aimed at designing a waste-to-energy process that converts waste tires to methanol through two different pathways - WT-electrified and WT-conventional, with the ultimate objective of achieving near-zero carbon emissions. The study also compares the environmental impacts of these new processes with the traditional natural gas to methanol process. The findings from the simulation and techno-economic analysis consistently demonstrated that the WT-electrified process is superior to the WT-conventional method in several key areas.

In terms of energy efficiency, the WT-electrified process achieved 55.8%, slightly higher than the 54.6% efficiency of the WT-conventional process. This indicates that the WTE process is more effective at converting energy with 15% higher methanol production compared to WTC process.

From a life cycle analysis perspective, the WTE process significantly reduces GHG emissions. It achieves 84% reduction in GHG emissions compared to the conventional natural gas process and 60% less GHG emissions compared to the WTC process. These results highlight the potential environmental benefits of the WT-electrified process.

Finally, an economic analysis revealed that the WT-electrified process requires less capital investment. Specifically, it requires $145 million per year, which is significantly less than the $161 million per year needed for the WT-conventional process. For the minimum selling price, methanol from the WT-electrified process sells at $145/tonne cheaper than the WT-conventional methanol price. In terms of credit required for avoided GHG, the electrified process requires, on average three times less credit than the conventional process to make the minimum selling price of the WT process similar to the current market price of methanol. This suggests that the WT-electrified process could be a more economically feasible solution for converting waste tires to methanol.

The research indicates that the WT-electrified process holds promise as a more efficient, environmentally friendly, and cost-effective method for converting waste tires to methanol than the alternatives. It points to a future where waste-to-energy processes like this could play a vital role in reducing GHG emissions and managing waste.

Appendix

The dataset considered for LCA midpoint analysis of different electricity sources is outlined in Table A 1.

Table A 1: Dataset for different electricity source for mid-point analysis

Electricity Source	Location	Reference Process	Process UUID
Natural Gas electricity	Canada, Alberta	High voltage electricity production in a combined cycle natural gas power plant	83c210d0-67b4-325f-83ab-abbe937f9985
Nuclear Electricity	Canada, Ontario	High voltage electricity production in a pressurized heavy water reactor nuclear plant	e08ac139-2690-33a9-81b3-48dc70b753bd
Hydro Electricity	Canada, Quebec	High voltage electricity production through run of river in a hydro power plant	2228b986-6902-3207-a076-3a982f818610
Wind Electricity	Canada, Quebec	High voltage electricity production in an onshore wind power plant	787d88a7-ec90-30f5-ad0a-1fc466ec20e0

References

[1] "Electrification of the chemical industry." Accessed: Aug. 15, 2022. [Online]. Available: https://www.science.org/doi/10.1126/science.abb8061

[2] C. Chen, Y. Lu, and R. Banares-Alcantara, "Direct and indirect electrification of chemical industry using methanol production as a case study," *Applied Energy*, vol. 243, pp. 71–90, Jun. 2019, doi: 10.1016/j.apenergy.2019.03.184.

[3] I. Eryazici, N. Ramesh, and C. Villa, "Electrification of the chemical industry—materials innovations for a lower carbon future," *MRS Bulletin*, vol. 46, no. 12, pp. 1197–1204, Dec. 2021, doi: 10.1557/s43577-021-00243-9.

[4] Z. J. Schiffer and K. Manthiram, "Electrification and Decarbonization of the Chemical Industry," *Joule*, vol. 1, no. 1, pp. 10–14, Sep. 2017, doi: 10.1016/j.joule.2017.07.008.

[5] "2020-07-10-whitepaper-ihp-a4.pdf." Accessed: Sep. 07, 2022. [Online]. Available: https://www.sintef.no/globalassets/sintef-energi/industrial-heat-pump-whitepaper/2020-07-10-whitepaper-ihp-a4.pdf

[6] "heatpump.pdf." Accessed: Sep. 02, 2022. [Online]. Available: https://www.energy.gov/sites/prod/files/2014/05/f15/heatpump.pdf

[7] S. J. Cooper, G. P. Hammond, N. Hewitt, J. B. Norman, S. A. Tassou, and W. Youssef, "Energy saving potential of high temperature heat pumps in the UK Food and Drink sector," *Energy Procedia*, vol. 161, pp. 142–149, Mar. 2019, doi: 10.1016/j.egypro.2019.02.073.

[8] S. Ai, B. Wang, X. Li, and W. Shi, "Comparison of mechanical vapor recompression technology for solution regeneration in heat-source tower heat pumps," *Building Services Engineering Research and Technology*, vol. 40, no. 3, pp. 360–378, May 2019, doi: 10.1177/0143624418817461.

[9] G. Liu *et al.*, "Performance of MVR desalination system with variable operating conditions for wastewater treatment," *DWT*, vol. 178, pp. 21–31, 2020, doi: 10.5004/dwt.2020.24983.

[10] O. Roelofsen, K. Somers, E. Speelman, and M. Witteveen, "Plugging in: What electrification can do for industry," p. 7.

[11] J. Moore *et al.*, "Chapter 9 - Compressors and expanders," in *Machinery and Energy Systems for the Hydrogen Economy*, K. Brun and T. Allison, Eds., Elsevier, 2022, pp. 333–424. doi: https://doi.org/10.1016/B978-0-323-90394-3.00002-3.

[12] Y. K. Salkuyeh, B. A. Saville, and H. L. MacLean, "Techno-economic analysis and life cycle assessment of hydrogen production from natural gas using current and emerging technologies," *International Journal of Hydrogen Energy*, vol. 42, no. 30, pp. 18894–18909, 2017, doi: https://doi.org/10.1016/j.ijhydene.2017.05.219.

[13] S. T. Wismann *et al.*, "Electrified methane reforming: A compact approach to greener industrial hydrogen production," *Science*, vol. 364, no. 6442, pp. 756–759, May 2019, doi: 10.1126/science.aaw8775.

[14] "Plasma (physics)," *Wikipedia*. Aug. 05, 2022. Accessed: Aug. 09, 2022. [Online]. Available: https://en.wikipedia.org/w/index.php?title=Plasma_(physics)&oldid=1102572089

[15] M. T. Munir, I. Mardon, S. Al-Zuhair, A. Shawabkeh, and N. U. Saqib, "Plasma gasification of municipal solid waste for waste-to-value processing," *Renewable and Sustainable Energy Reviews*, vol. 116, p. 109461, Dec. 2019, doi: 10.1016/j.rser.2019.109461.

[16] G. S. J. Sturm, A. N. Munoz, P. V. Aravind, and G. D. Stefanidis, "Microwave-Driven Plasma Gasification for Biomass Waste Treatment at Miniature Scale," *IEEE Trans. Plasma Sci.*, vol. 44, no. 4, pp. 670–678, Apr. 2016, doi: 10.1109/TPS.2016.2533363.

[17] A. Amini, M. Latifi, and J. Chaouki, "Electrification of materials processing via microwave irradiation: A review of mechanism and applications," *Applied Thermal Engineering*, vol. 193, p. 117003, Jul. 2021, doi: 10.1016/j.applthermaleng.2021.117003.

[18] P. Lahijani, Z. A. Zainal, A. R. Mohamed, and M. Mohammadi, "Microwave-enhanced CO2 gasification of oil palm shell char," *Bioresource Technology*, vol. 158, pp. 193–200, Apr. 2014, doi: 10.1016/j.biortech.2014.02.015.

[19] "2019 USTMA Scrap Tire Management Summary Report.pdf." Accessed: Oct. 06, 2022. [Online]. Available: https://www.ustires.org/sites/default/files/2019%20USTMA%20Scrap%20Tire%20Management%20Summary%20Report.pdf

[20] "CATRA_AR_2021_-_ENG.pdf." Accessed: Jul. 30, 2022. [Online]. Available: https://www.catraonline.ca/storage/files/shares/publications-en/CATRA_AR_2021_-_ENG.pdf

[21] A. Quek and R. Balasubramanian, "Liquefaction of waste tires by pyrolysis for oil and chemicals—A review," *Journal of Analytical and Applied Pyrolysis*, vol. 101, pp. 1–16, May 2013, doi: 10.1016/j.jaap.2013.02.016.

[22] C. Berrueco, E. Esperanza, F. J. Mastral, J. Ceamanos, and P. García-Bacaicoa, "Pyrolysis of waste tyres in an atmospheric static-bed batch reactor: Analysis of the gases obtained," *Journal of Analytical and Applied Pyrolysis*, vol. 74, no. 1–2, pp. 245–253, Aug. 2005, doi: 10.1016/j.jaap.2004.10.007.

[23] "Vulcanization - Rubber as a natural product, Vulcanization and properties of vulcanized rubber." Accessed: Oct. 19, 2021. [Online]. Available: https://science.jrank.org/pages/7266/Vulcanization.html

[24] "Publications | U.S. Tire Manufacturers Association." Accessed: Oct. 21, 2021. [Online]. Available: https://www.ustires.org/publications

[25] A. Fazli and D. Rodrigue, "Recycling Waste Tires into Ground Tire Rubber (GTR)/Rubber Compounds: A Review," *J. Compos. Sci.*, vol. 4, no. 3, p. 103, Jul. 2020, doi: 10.3390/jcs4030103.

[26] P. T. Williams, "Pyrolysis of waste tyres: A review," *Waste Management*, vol. 33, no. 8, pp. 1714–1728, Aug. 2013, doi: 10.1016/j.wasman.2013.05.003.

[27] J. Zebala, P. Ciepka, A. Reza, and R. Janczur, "Influence of rubber compound and tread pattern of retreaded tyres on vehicle active safety," *Forensic Science International*, vol. 167, no. 2–3, pp. 173–180, Apr. 2007, doi: 10.1016/j.forsciint.2006.06.051.

[28] H.-H. Tsang, "USES OF SCRAP RUBBER TIRES," p. 16.

[29] "paper6.pdf."

[30] S. Singh, W. Nimmo, B. M. Gibbs, and P. T. Williams, "Waste tyre rubber as a secondary fuel for power plants," *Fuel*, vol. 88, no. 12, pp. 2473–2480, Dec. 2009, doi: 10.1016/j.fuel.2009.02.026.

[31] Y. Fang, W. Li, and S. You, "Chapter 17 - Techno-economic analysis of biomass thermochemical conversion to biofuels," in *Value-Chain of Biofuels*, S. Yusup and N. A. Rashidi, Eds., Elsevier, 2022, pp. 379–394. doi: 10.1016/B978-0-12-824388-6.00023-3.

[32] A. R. K. Gollakota, N. Kishore, and S. Gu, "A review on hydrothermal liquefaction of biomass," *Renewable and Sustainable Energy Reviews*, vol. 81, pp. 1378–1392, Jan. 2018, doi: 10.1016/j.rser.2017.05.178.

[33] S. S. Toor, L. Rosendahl, and A. Rudolf, "Hydrothermal liquefaction of biomass: A review of subcritical water technologies," *Energy*, vol. 36, no. 5, pp. 2328–2342, May 2011, doi: 10.1016/j.energy.2011.03.013.

[34] A. Molino, S. Chianese, and D. Musmarra, "Biomass gasification technology: The state of the art overview," *Journal of Energy Chemistry*, vol. 25, no. 1, pp. 10–25, Jan. 2016, doi: 10.1016/j.jechem.2015.11.005.

[35] G. Song, S. Zhao, X. Wang, X. Cui, H. Wang, and J. Xiao, "An efficient biomass and renewable power-to-gas process integrating electrical heating gasification," *Case Studies in Thermal Engineering*, vol. 30, p. 101735, Feb. 2022, doi: 10.1016/j.csite.2021.101735.

[36] Q. Xie *et al.*, "Fast microwave-assisted catalytic gasification of biomass for syngas production and tar removal," *Bioresource Technology*, vol. 156, pp. 291–296, Mar. 2014, doi: 10.1016/j.biortech.2014.01.057.

[37] S. Kilpimaa, T. Kuokkanen, and U. Lassi, "Characterization and Utilization Potential of Wood Ash from Combustion Process and Carbon Residue from Gasification Process," *BioResources*, vol. 8, no. 1, pp. 1011–1027, Jan. 2013, doi: 10.15376/biores.8.1.1011-1027.

[38] A. Qayyum, U. Ali, and N. Ramzan, "Acid gas removal techniques for syngas, natural gas, and biogas clean up – a review," *Energy Sources, Part A: Recovery, Utilization, and Environmental Effects*, pp. 1–24, Aug. 2020, doi: 10.1080/15567036.2020.1800866.

[39] O. Ortíz-Rodríguez, W. Ocampo-Duque, and L. Duque-Salazar, "Environmental Impact of End-of-Life Tires: Life Cycle Assessment Comparison of Three Scenarios from a Case Study in Valle Del Cauca, Colombia," *Energies*, vol. 10, no. 12, p. 2117, Dec. 2017, doi: 10.3390/en10122117.

[40] A. S. R. Subramanian, T. Gundersen, and T. A. Adams, "Optimal design and operation of a waste tire feedstock polygeneration system," *Energy*, vol. 223, p. 119990, May 2021, doi: 10.1016/j.energy.2021.119990.

[41] M. C. Woods *et al.*, "Cost and performance baseline for fossil energy plants," *National Energy Technology Laboratory*, 2007.

[42] J. DeVincentis, "Physical Property Methods and Models 11.1".

[43] I. J. Okeke, "Design and systems-level performance analysis of petroleum coke conversion strategies".

[44] Y. K. Salkuyeh, A. Elkamel, J. Thé, and M. Fowler, "Development and techno-economic analysis of an integrated petroleum coke, biomass, and natural gas polygeneration process," *Energy*, vol. 113, pp. 861–874, Oct. 2016, doi: 10.1016/j.energy.2016.07.096.

[45] J. Haslback *et al.*, "Cost and Performance Baseline for Fossil Energy Plants, Volume 1: Bituminous Coal and Natural Gas to Electricity, Revision 2a," National Energy Technology

Laboratory (NETL), Pittsburgh, PA, Morgantown, WV, and Albany, OR (United States), DOE/NETL-2010/1397, Sep. 2013. doi: 10.2172/1513268.

[46] S. Michailos *et al.*, "Methanol worked examples for the TEA and LCA guidelines for CO2 utilization," 2018.

[47] "Methanol-Technical-Data-Sheet.pdf." Accessed: Sep. 13, 2023. [Online]. Available: https://www.methanol.org/wp-content/uploads/2016/06/Methanol-Technical-Data-Sheet.pdf

[48] Y. Khojasteh-Salkuyeh, O. Ashrafi, E. Mostafavi, and P. Navarri, "CO2 utilization for methanol production; Part I: Process design and life cycle GHG assessment of different pathways," *Journal of CO2 Utilization*, vol. 50, p. 101608, Aug. 2021, doi: 10.1016/j.jcou.2021.101608.

[49] "Air Products/Shell Gasifiers," netl.doe.gov. Accessed: Sep. 15, 2023. [Online]. Available: https://netl.doe.gov/research/carbon-management/energy-systems/gasification/gasifipedia/shell

[50] P. Mondal, G. S. Dang, and M. O. Garg, "Syngas production through gasification and cleanup for downstream applications — Recent developments," *Fuel Processing Technology*, vol. 92, no. 8, pp. 1395–1410, Aug. 2011, doi: 10.1016/j.fuproc.2011.03.021.

[51] Y. K. Salkuyeh and T. A. Adams, "A new power, methanol, and DME polygeneration process using integrated chemical looping systems," *Energy Conversion and Management*, vol. 88, pp. 411–425, Dec. 2014, doi: 10.1016/j.enconman.2014.08.039.

[52] C. Peinado *et al.*, "In Situ Conditioning of CO2-Rich Syngas during the Synthesis of Methanol," *Catalysts*, vol. 11, no. 5, 2021, doi: 10.3390/catal11050534.

[53] K. V. Bussche and G. F. Froment, "A steady-state kinetic model for methanol synthesis and the water gas shift reaction on a commercial Cu/ZnO/Al2O3Catalyst," *Journal of catalysis*, vol. 161, no. 1, pp. 1–10, 1996.

[54] E. Freireich and T. RN, "PROCESS IMPROVES ACID-GAS REMOVAL, TRIMS COSTS, AND REDUCES EFFLUENTS.," 1976.

[55] Y. K. Salkuyeh and M. Mofarahi, "Comparison of MEA and DGA performance for CO2 capture under different operational conditions," *Int. J. Energy Res.*, vol. 36, no. 2, pp. 259–268, Feb. 2012, doi: 10.1002/er.1812.

[56] B. Dutcher, M. Fan, and A. G. Russell, "Amine-Based CO2 Capture Technology Development from the Beginning of 2013—A Review," *ACS Appl. Mater. Interfaces*, vol. 7, no. 4, pp. 2137–2148, Feb. 2015, doi: 10.1021/am507465f.

[57] A. Marshall, B. Børresen, G. Hagen, M. Tsypkin, and R. Tunold, "Hydrogen production by advanced proton exchange membrane (PEM) water electrolysers—Reduced energy consumption by improved electrocatalysis," *Energy*, vol. 32, no. 4, pp. 431–436, 2007.

[58] P. Millet, N. Mbemba, S. Grigoriev, V. Fateev, A. Aukauloo, and C. Etiévant, "Electrochemical performances of PEM water electrolysis cells and perspectives," *International Journal of Hydrogen Energy*, vol. 36, no. 6, pp. 4134–4142, 2011.

[59] M. Carmo, D. L. Fritz, J. Mergel, and D. Stolten, "A comprehensive review on PEM water electrolysis," *International journal of hydrogen energy*, vol. 38, no. 12, pp. 4901–4934, 2013.

[60] G. Bozzano and F. Manenti, "Efficient methanol synthesis: Perspectives, technologies and optimization strategies," *Progress in Energy and Combustion Science*, vol. 56, pp. 71–105, 2016, doi: https://doi.org/10.1016/j.pecs.2016.06.001.

[61] K. Barati, Y. Khojasteh-Salkuyeh, O. Ashrafi, and P. Navarri, "Electrified combined reforming of methane process for more effective CO2 conversion to methanol: Process development and environmental impact assessment," *Energy Conversion and Management*, vol. 287, p. 117096, 2023, doi: https://doi.org/10.1016/j.enconman.2023.117096.

[62] V. Dieterich, A. Buttler, A. Hanel, H. Spliethoff, and S. Fendt, "Power-to-liquid via synthesis of methanol, DME or Fischer–Tropsch-fuels: a review," *Energy Environ. Sci.*, vol. 13, no. 10, pp. 3207–3252, 2020, doi: 10.1039/D0EE01187H.

[63] G. Leonzio, "Analysis and optimization of a methanol reactor with the adsorption of carbon monoxide and water," *Renewable Energy*, vol. 146, pp. 2744–2757, 2020, doi: https://doi.org/10.1016/j.renene.2019.08.084.

[64] M. R. Rahimpour, M. S. Baktash, B. Vaferi, and S. Mazinani, "Reduction in CO emissions along a two-stage hydrogen-permselective membrane reactor in methanol synthesis process," *Journal of Industrial and Engineering Chemistry*, vol. 17, no. 2, pp. 198–207, 2011, doi: https://doi.org/10.1016/j.jiec.2011.02.001.

[65] I. V. Muralikrishna and V. Manickam, "Life Cycle Assessment," in *Environmental Management*, Elsevier, 2017, pp. 57–75. doi: 10.1016/B978-0-12-811989-1.00005-1.

[66] C. E. R. Government of Canada, "CER – Provincial and Territorial Energy Profiles – Canada." Accessed: Sep. 20, 2023. [Online]. Available: https://www.cer-rec.gc.ca/en/data-

analysis/energy-markets/provincial-territorial-energy-profiles/provincial-territorial-energy-profiles-canada.html

[67] "Technical report - Comparing power generation options and electricity mixes".

[68] "LCIA-METHODS-v.1.5.5.pdf." Accessed: Aug. 27, 2023. [Online]. Available: https://www.openlca.org/wp-content/uploads/2016/08/LCIA-METHODS-v.1.5.5.pdf

[69] M. A. J. Huijbregts *et al.*, "ReCiPe2016: a harmonised life cycle impact assessment method at midpoint and endpoint level," *Int J Life Cycle Assess*, vol. 22, no. 2, pp. 138–147, Feb. 2017, doi: 10.1007/s11367-016-1246-y.

[70] L. Wang, Y. Wang, Z. Zhou, M. P. Garvlehn, and F. Bi, "Comparative Assessment of the Environmental Impacts of Hydro-Electric, Nuclear and Wind Power Plants in China: Life Cycle Considerations.," *Energy Procedia*, vol. 152, pp. 1009–1014, Oct. 2018, doi: 10.1016/j.egypro.2018.09.108.

[71] Q. Zhang, B. Karney, H. L. MacLean, and J. Feng, "Life-Cycle Inventory of Energy Use and Greenhouse Gas Emissions for Two Hydropower Projects in China," *J. Infrastruct. Syst.*, vol. 13, no. 4, pp. 271–279, Dec. 2007, doi: 10.1061/(ASCE)1076-0342(2007)13:4(271).

[72] "10.3. Syngas Conversion to Methanol," netl.doe.gov. Accessed: Sep. 06, 2023. [Online]. Available: https://www.netl.doe.gov/research/carbon-management/energy-systems/gasification/gasifipedia/methanol

[73] "Industrial electricity prices in major Canadian cities," Statista. Accessed: Sep. 11, 2023. [Online]. Available: https://www.statista.com/statistics/579159/average-industrial-electricity-prices-canada-by-major-city/

[74] "Pricing," Methanex. Accessed: Jun. 26, 2023. [Online]. Available: https://www.methanex.com/about-methanol/pricing/

[75] T. A. Adams II and P. I. Barton, "Combining coal gasification and natural gas reforming for efficient polygeneration," *Fuel Processing Technology*, vol. 92, no. 3, pp. 639–655, 2011.

[76] S. Jenkins, "2022 CEPCI updates: December (prelim.) and November (final)," Chemical Engineering. Accessed: Jun. 26, 2023. [Online]. Available: https://www.chemengonline.com/2022-cepci-updates-december-prelim-and-november-final/

[77] M. S. Peters, K. D. Timmerhaus, and R. E. West, *Plant Design and Economics for Chemical Engineers*. in McGraw-Hill chemical engineering series. McGraw-Hill Education, 2003. [Online]. Available: https://books.google.ca/books?id=yNZTAAAAMAAJ

[78] R. Smith, "Chemical Process Design and Integration".

[79] D. W. Green and M. Z. Southard, Eds., *Perry's Chemical Engineers' Handbook*, 9th Edition. New York: McGraw-Hill Education, 2019. [Online]. Available: https://www.accessengineeringlibrary.com/content/book/9780071834087

[80] W. D. Seider, D. R. Lewin, J. D. Seader, S. Widagdo, R. Gani, and K. M. Ng, *Product and Process Design Principles: Synthesis, Analysis, and Evaluation*. John Wiley & Sons Incorporated, 2017. [Online]. Available: https://books.google.ca/books?id=73eijwEACAAJ

[81] F. Benaskar *et al.*, "Cost Analysis for a Continuously Operated Fine Chemicals Production Plant at 10 Kg/Day Using a Combination of Microprocessing and Microwave Heating," *Journal of Flow Chemistry*, vol. 1, no. 2, pp. 74–89, Dec. 2011, doi: 10.1556/jfchem.2011.00015.